

Early Detection of Misinformation for Infodemic Management: A Domain Adaptation Approach

Minjia Mao
University of Delaware

Xiaohang Zhao*
Shanghai University of Finance and Economics

Xiao Fang*
University of Delaware

*Corresponding author

Abstract. An infodemic refers to an enormous amount of true information and misinformation disseminated during a disease outbreak. Detecting misinformation at the early stage of an infodemic is key to manage it and reduce its harm to public health. An early stage infodemic is characterized by a large volume of unlabeled information concerning a disease. As a result, conventional misinformation detection methods are not suitable for this misinformation detection task because they rely on labeled information in the infodemic domain to train their models. To address the limitation of conventional methods, state-of-the-art methods learn their models using labeled information in other domains to detect misinformation in the infodemic domain. The efficacy of these methods depends on their ability to mitigate both covariate shift and concept shift between the infodemic domain and the domains from which they leverage labeled information. These methods focus on mitigating covariate shift but overlook concept shift, rendering them less effective for the task. In response, we theoretically show the necessity of tackling both covariate shift and concept shift as well as how to operationalize each of them. Built on the theoretical analysis, we develop a novel misinformation detection method that addresses both covariate shift and concept shift. Using two real-world datasets, we conduct extensive empirical evaluations to demonstrate the superior performance of our method over state-of-the-art misinformation detection methods as well as prevalent domain adaptation methods that can be tailored to solve the misinformation detection task.

Key words: misinformation detection, infodemic management, domain adaptation, covariate shift, concept shift, deep learning, contrastive learning, transfer learning

1. Introduction

An infodemic refers to an overwhelming volume of true and false information spread during a disease outbreak (Van Der Linden 2022). Misinformation, or false information, in an infodemic misleads the public about the disease and causes significant harm to public health (Imhoff and Lamberty 2020, Freeman et al. 2022, Van Der Linden 2022). For example, the misinformation that the Ebola virus is intentionally created by the Congolese government to eliminate people in the city of Beni has led to attacks on Ebola clinics by local residents, hindering timely treatments for Ebola.¹ More recently, during the outbreak of the

¹ See <https://news.un.org/en/story/2019/03/1034381> (last accessed on May 28, 2024)

coronavirus disease (COVID-19), a significant amount of misinformation has been diffused on social media. Examples include the misinformation that baking soda can cure coronavirus,² the false claim that injecting disinfectant can prevent the virus (Borah et al. 2022), and the incorrect attribution of the outbreak in Italy to Middle East illegal immigrants.³ Such widespread of misinformation about COVID-19 has caused social panic, led people to dismiss health guidance, and weakened their confidence in vaccines, ultimately undermining pandemic response efforts (Bursztyrn et al. 2020). Therefore, it is imperative to manage an infodemic to mitigate its adverse impact on public health (Freeman et al. 2022, Hwang and Lee 2024).

According to the World Health Organization (WHO), infodemic management is the use of risk- and evidence-based approaches to manage an infodemic and reduce its harm to public health.⁴ The key to effective infodemic management is the detection of misinformation at the early stage of an infodemic (Buchanan 2020, Van Der Linden 2022). Early identification of misinformation discourages people from sharing it and prevents it from reaching a much larger population, thereby mitigating its potential harm to public health (Buchanan 2020). Moreover, the likelihood that a person trusts misinformation increases as the person is exposed longer to the misinformation (Zajonc 2001, Moravec et al. 2019). Early identification of misinformation reduces individuals' exposure time to misinformation, thereby lowering their likelihoods of trusting it. This, in turn, increases their chances of adhering to health guidance, ultimately benefiting public health as a whole.

An early stage infodemic features two salient characteristics. First, an emerging health event triggers a huge amount of true and false information spreading on various media platforms in a short time period. For example, during the early stage of the COVID-19 infodemic, a significant volume of true and false information concerning COVID-19 is diffused on social media (Yue et al. 2022), and the WHO declares a worldwide infodemic (Van Der Linden 2022). Second, it requires expert knowledge to distinguish between true information and misinformation in an infodemic. Moreover, during the early stage of a disease outbreak and its ensuing infodemic, even experts have no or limited knowledge about the disease, making it even more difficult to discern true information from misinformation. For example, during the early stage of the Ebola outbreak, scientists lack knowledge about the disease and its treatment (Adebimpe et al. 2015). Consequently, it is common that information disseminated at the early stage of an infodemic is unlabeled. As there is no labeled information (i.e., true or false), it is impossible to learn a misinformation detection model using conventional misinformation detection methods such as Abbasi et al. (2010), Nan et al. (2021), and Wei et al. (2022), which require labeled information in their training data.

² See <https://apnews.com/article/archive-fact-checking-8736262219> (last accessed on May 28, 2024)

³ See <https://time.com/5789666/italy-coronavirus-far-right-salvini/> (last accessed on May 28, 2024)

⁴ See https://www.who.int/health-topics/infodemic#tab=tab_1 (last accessed on May 28, 2024)

A viable solution is to leverage labeled information in other domains to build a misinformation detection model for the infodemic domain. Indeed, popular fact-checking websites like PolitiFact⁵ and Gossipcop⁶ contain a wealth of verified true and false information in domains such as politics and entertainment. Moreover, misinformation across domains shares some common characteristics. For example, compared to true information, misinformation spreads faster, farther, and more widely (Oh et al. 2013, Vosoughi et al. 2018). As another example, fake news, an important type of misinformation, often features emotional headlines and demonstrates inconsistency between their headlines and contents (Siering et al. 2016). Because of these common characteristics shared across domains, it is possible to learn a misinformation detection model using labeled information in other domains and transfer it to the infodemic domain. However, information in each domain also has its unique characteristics. Understandably, the choice of words and the organization of words to convey sentiments and semantics differ across domains. For example, less than 20% of words used in politics news overlaps with those found in entertainment news (Shu et al. 2020). Because each domain possesses unique characteristics, a misinformation detection model learned with labeled information in other domains usually performs poorly in the infodemic domain.

Domain adaptation is a widely employed technique to enhance the performance of a model trained in one domain but applied to another (Ben-David et al. 2010). It aims to mitigate disparities between data in different domains such that a model learned using data in one domain performs well in another domain (Ben-David et al. 2010). Concretely, data in a domain is represented as a joint distribution $p(\mathbf{x}, y)$, $\mathbf{x} \in \mathcal{X}$, $y \in \mathcal{Y}$, where \mathcal{X} denotes the feature space and \mathcal{Y} is the label space (Liu et al. 2022). In the context of misinformation detection, \mathbf{x} might be explicit features, such as the number of words in a piece of information, or latent features, such as the embedding of a piece of information (Zhou and Zafarani 2020). Label y denotes whether a piece of information is true or false. The joint distribution $p(\mathbf{x}, y)$ can be expressed as the product of $p(\mathbf{x})$ and $p(y|\mathbf{x})$, i.e., $p(\mathbf{x}, y) = p(\mathbf{x})p(y|\mathbf{x})$. Accordingly, to effectively alleviate disparities between data in different domains, it is essential to reduce both their differences in terms of $p(\mathbf{x})$ and their differences in terms of $p(y|\mathbf{x})$, where the former type of differences is referred to as *covariate shift* and the latter type of differences is known as *concept shift* (Liu et al. 2022). Existing domain adaptation methods focus on mitigating covariate shift between domains (Ganin et al. 2016, Long et al. 2017, Zhu et al. 2019, Peng et al. 2019). By applying these domain adaptation methods, Huang et al. (2021), Li et al. (2021), Yue et al. (2022) develop state-of-the-art misinformation detection methods, which learn a model from labeled information in one or more source domains to identify misinformation in a target domain with no labeled information. Although these misinformation detection methods are applicable to our problem, their efficacy is limited because they fail to account for concept shift.

⁵ See <https://www.politifact.com/> (last accessed on May 28, 2024)

⁶ See https://en.wikipedia.org/wiki/Gossip_Cop (last accessed on May 28, 2024)

In response to the research gaps, this study contributes to the literature with a novel misinformation detection method that tackles both covariate shift and concept shift. Our method design is rooted in our theoretical analysis, which shows the necessity of addressing both covariate shift and concept shift for effective domain adaptation as well as how to operationalize each of them. Guided by the theoretical analysis, we develop two modules in our method: one for assessing and reducing covariate shift and the other for evaluating and mitigating concept shift. Therefore, the primary methodological difference between our method and state-of-the-art domain adaptation-based misinformation detection methods (e.g., Yue et al. (2022)) is the addressing of concept shift by our method. It also differs from conventional misinformation detection methods such as Wei et al. (2022). Specifically, our method is a cross-domain method that learns a model from labeled information in other domains to classify unlabeled information in the infodemic domain. In contrast, conventional misinformation detection methods are single-domain methods that learn a model from labeled information in a domain (e.g., infodemic domain) to classify unlabeled information in the same domain.

2. Related Work

Existing methods for misinformation detection can be classified into three categories: single-domain, multi-domain, and cross-domain approaches. In this section, we review each category of these methods and highlight the methodological novelty of our study.

2.1. Single and Multi-domain Misinformation Detection Methods

Single-domain misinformation detection methods train a classification model using labeled information from a specific domain (e.g., true and fake news from the domain of politics), and then employ the model to classify unlabelled information in the same domain (e.g., unlabelled political news). In this category, knowledge-based methods classify unlabelled information by comparing the content of the information (e.g., textual content of news) against known facts (Ciampaglia et al. 2015). More specifically, these methods retrieve pertinent facts from authoritative websites like Wikipedia, represent extracted facts as a knowledge graph, and employ the knowledge graph to automatically detect misinformation. Additionally, writing styles identified from the content of information, such as readability, sensationalism, informality, and subjectivity, have been utilized to detect misinformation (Zhou and Zafarani 2020). Recent methods consider the propagation of information on social media, in addition to the content of information (Papanastasiou 2020). Some methods employ propagation patterns to detect misinformation because misinformation spreads faster, farther, and more widely compared to true information (Vosoughi et al. 2018). Others harness the collective intelligence of crowds, such as likes, shares, and comments from social media users (Atanasov et al. 2017, Pennycook and Rand 2021). For example, Wei et al. (2022) employ both the content of news articles and social media users' comments on these news articles to detect fake news.

Multi-domain misinformation detection methods learn a classification model from labeled information in various domains (e.g., true and fake news in the politics, health, and sports domains), and then employ the model to classify unlabelled information in each of these domains (Nan et al. 2021, Zhu et al. 2023). The rationale underlying these methods is to leverage labeled information in multiple domains to enhance misinformation detection in each individual domain. However, because of variations in information content among different domains, a model learned with labeled information in these domains exhibits significant performance differences when applied to each of these domains (Zhu et al. 2023). That is, the effectiveness of the learned model in identifying misinformation in one domain could be significantly inferior to its effectiveness in detecting misinformation in another domain. To tackle this problem, several methods incorporate domain-specific characteristics into the model training. For example, Nan et al. (2021) propose to embed different domains as different vectors and integrate these vectors into the learning of a multi-domain misinformation detection model. Zhu et al. (2023) introduce domain adapters tailored to each specific domain; representations of news articles in each domain are then adjusted by their corresponding domain adapter to train a multi-domain model.

2.2. Cross-domain Misinformation Detection Methods

Cross-domain misinformation detection methods leverage labeled information in one or more source domains (e.g., true and fake news in the politics and sports domains) to classify unlabelled information in a target domain (e.g., unlabelled news in the health domain). Unlike multi-domain methods, which identify misinformation in various domains, cross-domain methods focus on detecting misinformation in one target domain. Depending on whether training data contain labeled or unlabeled information in a target domain, cross-domain methods can be further categorized into two subgroups.

One subgroup of cross-domain methods learns a model from training data consisting of labeled information in source domains as well as labeled information in a target domain to classify unlabeled information in the target domain (Mosallanezhad et al. 2022, Nan et al. 2022). These methods essentially utilize labeled source domain information as out-of-distribution data to improve the performance of misinformation detection in the target domain (Zhang et al. 2023). For example, Nan et al. (2022) pretrain a misinformation detection model using labeled information in source and target domains. Next, a language model is learned from labeled target domain information. Each piece of source domain information is then assigned a transferability score based on the degree to which the language model can predict its content. Finally, the pretrained model is fine-tuned using labeled source domain information weighted by their corresponding transferability scores as well as labeled target domain information.

The other subgroup learns a model from training data consisting of labeled information in source domains and unlabeled information in a target domain. Since there is no labeled target domain information, this subgroup of methods aims to transfer a model learned from labeled source domain information to the target

domain. To this end, domain adaptation is a suitable and widely adopted technique. In the following, we review domain adaptation methods and their applications in cross-domain misinformation detection. In the literature of domain adaptation, a domain consists of a feature space \mathcal{X} , a label space \mathcal{Y} , and a probability distribution $p(\mathbf{x}, y)$, $\mathbf{x} \in \mathcal{X}$ and $y \in \mathcal{Y}$ (Liu et al. 2022). As the probability distribution in a source domain usually differs from that in a target domain, a model learned from source domain data often performs poorly in the target domain (Ben-David et al. 2010). To tackle this issue, it is necessary to reduce the disparity between source and target domains in terms of $p(\mathbf{x}, y)$. Existing domain adaptation methods concentrate on mitigating the difference in feature distribution (i.e., $p(\mathbf{x})$) between source and target domains, known as covariate shift (Kouw and Loog 2018).⁷ In this vein, Ganin et al. (2016) propose a domain adversarial network to learn domain-invariant features from data in source and target domains. Saito et al. (2018) devise a mini-max mechanism to align feature distributions between source and target domains. In the maximum stage, two classifiers are learned from source samples such that the discrepancy between their classifications of target samples is maximized. In the minimum stage, features of target samples are adjusted to minimize such discrepancy. Rangwani et al. (2022) develop a domain adaptation method that incorporates a smoothing mechanism into the method proposed by Ganin et al. (2016). Rostami and Galstyan (2023) construct a pseudo-dataset using a model learned from labeled source domain data and then mitigate feature distribution difference between the pseudo-dataset and target domain data.⁸ While the methods reviewed above implicitly minimize covariate shift between source and target domains, there are methods explicitly measure and minimize covariate shift. For example, Long et al. (2015) utilize a metric known as the multi-kernel Maximum Mean Discrepancy (MMD) to quantify covariate shift, integrate this metric into a loss function, and minimize covariate shift by minimizing the loss function. In a follow-up study, Long et al. (2017) introduce another metric, known as the joint MMD, to measure covariate shift. In addition, Chen et al. (2022) employ the nuclear-norm Wasserstein discrepancy to evaluate covariate shift between source and target domains. Recent studies have employed domain adaptation techniques to solve the cross-domain misinformation detection problem with unlabeled target domain information. For example, Li et al. (2021) extend the work of Ganin et al. (2016) to detect misinformation in a target domain by leveraging labeled information in multiple source domains whereas Ng et al. (2023) apply the domain adversarial network

⁷ In the field of data stream mining, concept shift or concept drift refers to the phenomenon that data samples with same features could have different labels at different timestamps (Agrahari and Singh 2022, Roychowdhury et al. 2023). Given a model trained with previous data samples and a continuous influx of new data samples, the objective of data stream mining methods is to determine when and how to retrain the model (Vorburger and Bernstein 2006, Fang et al. 2013, Agrahari and Singh 2022, Roychowdhury et al. 2023). These methods are not applicable to our problem because they require labeled data samples at all timestamps while instances of target domain information are unlabeled in our problem. Moreover, these methods aim to decide when and how to retrain a model in a dynamic environment, whereas the objective of our problem is to classify unlabeled target domain instances.

⁸ Although the title of the paper contains the phrase of concept shift, it actually mitigates covariate shift. This is evident in the objective function of the proposed algorithm, i.e., Equation (3) in (Rostami and Galstyan 2023). According to the equation, the algorithm aims to mitigate the difference between the feature distribution $p_T(\mathbf{X}_T)$ of target domain data and the feature distribution $\hat{p}_J(\mathbf{Z}_p)$ of the pseudo-dataset.

Table 1 Comparison Between Our Method and Existing Misinformation Detection Methods.

	Applicable to our problem	Addressing covariate shift	Addressing concept shift
Single- and multi-domain misinformation detection methods, e.g., Wei et al. (2022), Zhu et al. (2023)	No	No	No
Cross-domain misinformation detection methods with labeled target domain information, e.g., Mosallanezhad et al. (2022), Nan et al. (2022)	No	Yes	No
Cross-domain misinformation detection methods with unlabeled target domain information, e.g., Li et al. (2021), Yue et al. (2022)	Yes	Yes	No
Our method	Yes	Yes	Yes

developed by (Ganin et al. 2016) to identify fake news and reviews. Huang et al. (2021) utilize the MMD metric to measure covariate shift between source domain information and target domain information, and mitigate covariate shift by minimizing the metric. Yue et al. (2022) develop a variant of the MMD metric to measure covariate shift between source and target domain information.

2.3. Key Novelty of Our Study

Our literature review suggests the following research gaps, as summarized in Table 1. First, existing single and multi-domain misinformation detection methods as well as cross-domain methods with labeled target domain information are not applicable to our problem. These methods require labeled target domain information (i.e., the infodemic domain in our study) in their training datasets, while our problem involves completely unlabeled information in the infodemic domain. Second, although existing cross-domain methods with unlabeled target domain information are applicable to our problem, they are less effective in solving the problem because they fail to address concept shift. In fact, none of the existing misinformation detection methods is capable of tackling concept shift. However, to ensure the efficacy of a model learned using labeled source domain information in classifying unlabeled target domain information, it is essential to mitigate both covariate shift and concept shift between source and target domains (Liu et al. 2022). To this end, we propose a misinformation detection method that tackles both covariate shift and concept shift, in contrast to existing methods that focus on covariate shift solely. Therefore, the key methodological novelty of our method lies in its addressing of concept shift. To implement this methodological novelty, our study features two innovations. First, our theoretical analysis of domain adaptation not only underscores the importance of addressing both covariate shift and concept shift but also shows how to operationalize each of them. Second, informed by our theoretical analysis, we introduce a novel misinformation detection method, two modules of which are respectively designed to tackle covariate shift and concept shift.

3. Problem Formulation

We consider a misinformation detection problem at the early stage of an infodemic, when all instances of information in this domain are unlabeled. Concretely, let \mathcal{D}_T be a dataset of N_T pieces of unlabeled information in the infodemic domain. The subscript T signifies target domain, which is the infodemic domain in this study. As an example, a piece of unlabeled information might encompass the textual content of a news article about COVID-19. Let \mathbf{x}_i^T denote a set of features extracted from a piece of unlabeled information in \mathcal{D}_T , $i = 1, 2, \dots, N_T$. We aim to predict the label (true or false) for each piece of information in \mathcal{D}_T .

To accomplish this objective, we are given k datasets of labeled information, i.e., $\mathcal{D}_{S_1}, \mathcal{D}_{S_2}, \dots, \mathcal{D}_{S_k}$. The subscript S refers to source domain, which provides labeled information to facilitate the label prediction in the target domain. Concretely, \mathcal{D}_{S_j} consists of N_{S_j} pieces of labeled information, $j = 1, 2, \dots, k$. Considering an example of S_j being the politics domain, a piece of information in this domain could comprise the textual content of a political news article. Each piece of labeled information in \mathcal{D}_{S_j} is represented as $(\mathbf{x}_i^{S_j}, y_i^{S_j})$, where $\mathbf{x}_i^{S_j}$ denotes features extracted from the information, $y_i^{S_j}$ is the label of the information, and $i = 1, 2, \dots, N_{S_j}$. Label $y_i^{S_j} = 0$ indicates that the information is true and $y_i^{S_j} = 1$ shows that the information is false. We now formally define the problem of early detection of misinformation for infodemic management.

Definition 1 (Early Detection of Misinformation Problem (EDM)). Given a dataset \mathcal{D}_T of N_T pieces of unlabeled information in the infodemic domain and k datasets of labeled information in various source domains, $\mathcal{D}_{S_1}, \mathcal{D}_{S_2}, \dots, \mathcal{D}_{S_k}$, where \mathcal{D}_{S_j} consists of N_{S_j} pieces of labeled information, $j = 1, 2, \dots, k$, the objective of the problem is to learn a model from the data to classify each piece of information in \mathcal{D}_T as true or false.

4. Method

In this section, we theoretically analyze the performance of a model learned using labeled source domain instances but applied to classify unlabeled target domain instances. Guided by the insights from our theoretical analysis, we then propose a novel method to solve the EDM problem.

4.1. Theoretical Analysis

We start with the setting of one target domain T and one source domain S . Let \mathcal{D}_T be a dataset of N_T unlabelled instances in T and \mathcal{D}_S be a dataset of N_S labeled instances in S . In the context of misinformation detection, an instance is a piece of information. We denote f_T as the true labeling function in the target domain that maps an instance with features \mathbf{x} into the probability of the instance being 1, i.e., $f_T(\mathbf{x}) = p_T(y = 1|\mathbf{x})$. Similarly, f_S is the true labeling function in the source domain and $f_S(\mathbf{x}) = p_S(y = 1|\mathbf{x})$. Let h be a hypothesis learned from labeled instances in \mathcal{D}_S and $h(\mathbf{x}) = p_h(y = 1|\mathbf{x})$. Following Ben-David et al.

(2010), we define the source error $\epsilon_S(h)$ of hypothesis h as the expected difference between h and the true labeling function f_S in the source domain

$$\epsilon_S(h) = E_{\mathbf{x} \sim \mathbb{D}_S} [|h(\mathbf{x}) - f_S(\mathbf{x})|], \quad (1)$$

where \mathbb{D}_S represents the feature distribution in the source domain. In a similar manner, we define the target error $\epsilon_T(h)$ of hypothesis h as the expected difference between h and the true labelling function f_T in the target domain

$$\epsilon_T(h) = E_{\mathbf{x} \sim \mathbb{D}_T} [|h(\mathbf{x}) - f_T(\mathbf{x})|], \quad (2)$$

where \mathbb{D}_T denotes the feature distribution in the target domain. Recall that domain adaptation aims to learn h from labeled instances in \mathcal{D}_S to classify each unlabelled instance in \mathcal{D}_T . Thus, the objective of domain adaptation is to minimize the target error $\epsilon_T(h)$. To achieve this objective, we show a bound of $\epsilon_T(h)$ in the following theorem.

Theorem 1 *For a source domain instance with features \mathbf{x}_i^S , let $c(\mathbf{x}_i^S)$ be the features of its nearest target domain instance, where $i = 1, 2, \dots, N_S$ and the distance between a pair of instances are measured over their feature space. If f_T is L -Lipschitz continuous,⁹ then for any $\eta \in (0, 1)$, with probability at least $(1 - \eta)^2$,*

$$\epsilon_T(h) \leq \epsilon_S(h) + \hat{d}_{\mathcal{H}}(\mathcal{D}_S, \mathcal{D}_T) + \frac{1}{N_S} \sum_{i=1}^{N_S} |f_S(\mathbf{x}_i^S) - f_T(c(\mathbf{x}_i^S))| + \frac{L}{N_S} \sum_{i=1}^{N_S} \|\mathbf{x}_i^S - c(\mathbf{x}_i^S)\| + C_1, \quad (3)$$

where L is the Lipschitz constraint constant, C_1 is a constant, $\hat{d}_{\mathcal{H}}(\mathcal{D}_S, \mathcal{D}_T)$ denotes the empirical \mathcal{H} -divergence between distributions \mathbb{D}_S and \mathbb{D}_T , estimated using features of source domain instances in \mathcal{D}_S and features of target domain instances in \mathcal{D}_T , and $\|\mathbf{x}_i^S - c(\mathbf{x}_i^S)\|$ represents the distance between \mathbf{x}_i^S and $c(\mathbf{x}_i^S)$.

Proof. See Appendix B.

Theorem 1 establishes an upper bound of $\epsilon_T(h)$, which can be empirically computed using datasets \mathcal{D}_S and \mathcal{D}_T drawn from distributions \mathbb{D}_S and \mathbb{D}_T , respectively. By Theorem 1, to minimize $\epsilon_T(h)$, we need to minimize the first three terms of its upper bound specified in Inequality (3). This is because the fourth term of the upper bound is inherently minimized, given that $c(\mathbf{x}_i^S)$ is the closest to \mathbf{x}_i^S , and the last term C_1 is a constant.

The first term $\epsilon_S(h)$ can be minimized by learning a classification model from labeled source domain instances. The second term $\hat{d}_{\mathcal{H}}(\mathcal{D}_S, \mathcal{D}_T)$ is the empirical estimation of the \mathcal{H} -divergence between the source domain feature distribution \mathbb{D}_S and the target domain feature distribution \mathbb{D}_T . \mathcal{H} -divergence has

⁹ The L -Lipschitz continuous assumption is commonly used in theoretical analyses of machine learning algorithms (e.g., Arjovsky et al. 2017, Asadi et al. 2018, Kim et al. 2021).

been extensively utilized in domain adaptation studies to measure distances between distributions. Please refer to Appendix A for a description of \mathcal{H} -divergence and its empirical estimation $\hat{d}_{\mathcal{H}}(\mathcal{D}_S, \mathcal{D}_T)$. Fundamentally, minimizing the \mathcal{H} -divergence between source and target domain feature distributions is to minimize covariate shift between source and target domains. Therefore, existing domain adaptation methods for mitigating covariate shift, such as Ganin et al. (2016) and Zhu et al. (2019), can be applied to minimize $\hat{d}_{\mathcal{H}}(\mathcal{D}_S, \mathcal{D}_T)$.

For the third term $\frac{1}{N_S} \sum_{i=1}^{N_S} |f_S(\mathbf{x}_i^S) - f_T(c(\mathbf{x}_i^S))|$, recall that $f_S(\mathbf{x}_i^S) = p_S(y = 1 | \mathbf{x}_i^S)$ and $f_T(c(\mathbf{x}_i^S)) = p_T(y = 1 | c(\mathbf{x}_i^S))$. Hence, to minimize the third term, we need to minimize the summation of differences between $p_S(y = 1 | \mathbf{x}_i^S)$ and $p_T(y = 1 | c(\mathbf{x}_i^S))$, summed over all source domain instances and their corresponding nearest target domain instances. Therefore, minimizing the third term is essentially to minimize concept shift between source and target domains.

Next, we consider the setting of one target domain T and multiple source domains S_1, S_2, \dots, S_k . Similar to the notations used in the setting of one source domain, we denote \mathcal{D}_T as a dataset of N_T unlabelled instances in T and \mathcal{D}_{S_j} as a dataset of N_{S_j} labeled instances in S_j , $j = 1, 2, \dots, k$. Let h be a hypothesis learned from labeled instances in $\mathcal{D}_{S_1}, \mathcal{D}_{S_2}, \dots, \mathcal{D}_{S_k}$. We denote f_T and f_{S_j} as the true labeling functions in T and S_j , respectively, $j = 1, 2, \dots, k$. For a hypothesis h , $\epsilon_T(h)$ and $\epsilon_{S_j}(h)$ represent its errors in T and S_j , respectively, $j = 1, 2, \dots, k$. Built on Theorem 1, the following proposition gives an upper bound of $\epsilon_T(h)$ in the setting of multiple source domains.

Proposition 1 *For a source domain instance with features $\mathbf{x}_i^{S_j}$ in \mathcal{D}_{S_j} , let $c(\mathbf{x}_i^{S_j})$ be the features of its nearest instance in \mathcal{D}_T , where $j = 1, 2, \dots, k$ and $i = 1, 2, \dots, N_{S_j}$. If f_T is L -Lipschitz continuous, then for any $\eta \in (0, 1)$, with probability at least $(1 - \eta)^{2k}$,*

$$\epsilon_T(h) \leq \frac{1}{k} \sum_{j=1}^k \{ \epsilon_{S_j}(h) + \hat{d}_{\mathcal{H}}(\mathcal{D}_{S_j}, \mathcal{D}_T) + \frac{1}{N_{S_j}} \sum_{i=1}^{N_{S_j}} |f_{S_j}(\mathbf{x}_i^{S_j}) - f_T(c(\mathbf{x}_i^{S_j}))| + \frac{L}{N_{S_j}} \sum_{i=1}^{N_{S_j}} \|\mathbf{x}_i^{S_j} - c(\mathbf{x}_i^{S_j})\| + C_j \}, \quad (4)$$

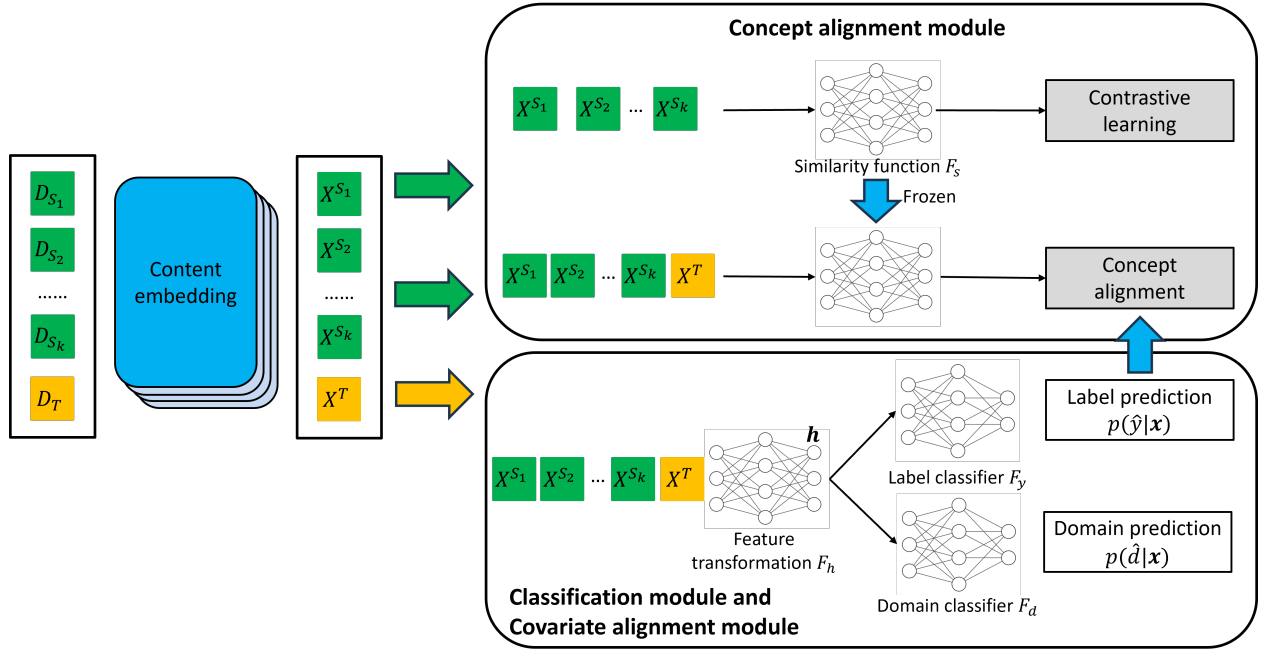
where L is the Lipschitz constraint constant, C_j is a constant, and $\hat{d}_{\mathcal{H}}(\mathcal{D}_{S_j}, \mathcal{D}_T)$ denotes the empirical \mathcal{H} -divergence between the feature distribution in the source domain S_j and that in the target domain T .

Proof. See Appendix B.

Proposition 1 offers useful insights for solving the EDM problem, which aims to learn a model from labeled information in multiple source domains to classify unlabeled information in the target infodemic domain with minimum error (i.e., $\epsilon_T(h)$). Informed by the proposition, we design a method that minimizes $\epsilon_T(h)$ through its three modules, each dedicated to reducing one of the first three terms in Inequality (4). Specifically, to reduce $\sum_{j=1}^k \epsilon_{S_j}(h)$, we implement a classification module, which is trained to accurately predict the label for each piece of source domain information. A covariate alignment module is developed to reduce $\sum_{j=1}^k \hat{d}_{\mathcal{H}}(\mathcal{D}_{S_j}, \mathcal{D}_T)$, thus diminishing covariate shift between source domains and the target

domain. Finally, we propose a concept alignment module to mitigate $\sum_{j=1}^k \sum_{i=1}^{N_{S_j}} |f_{S_j}(\mathbf{x}_i^{S_j}) - f_T(c(\mathbf{x}_i^{S_j}))|$, thereby reducing concept shift between source domains and the target domain. The concept alignment module constitutes the main methodological novelty of our method, and we designate our method as Domain Adaptation with Concept Alignment (DACA).

Figure 1 Overall Architecture of Domain Adaptation with Concept Alignment (DACA) Method



Note. Better view in color.

4.2. Method Overview

Grounded in our theoretical analysis, the DACA method adeptly alleviates disparities between source and target domains through its covariate alignment and concept alignment modules. As a result, the model learned from labeled source domain information by its classification module can effectively classify unlabeled infodemic domain information. Figure 1 illustrates the overall architecture of the DACA method. As shown, the inputs to the method consist of k datasets of labeled information in various source domains, $\mathcal{D}_{S_1}, \mathcal{D}_{S_2}, \dots, \mathcal{D}_{S_k}$, and a dataset \mathcal{D}_T of unlabeled information in the target infodemic domain. A content embedding function extracts features from the content of each piece of input information. Various content embedding functions (e.g., Kenton and Toutanova 2019, Zhu et al. 2023) could be used for this purpose, and we describe the content embedding function employed in this study in Section 5.2. Let $X^{S_j} = \{\mathbf{x}_i^{S_j} | i = 1, 2, \dots, N_{S_j}\}$ and $X^T = \{\mathbf{x}_i^T | i = 1, 2, \dots, N_T\}$ denote the set of features extracted from input information in source domain S_j and target domain T , respectively, $j = 1, 2, \dots, k$. These features serve as the inputs to the three modules of the DACA method.

The classification module trains a label classifier to accurately predict the label of a piece of information as either true (0) or false (1). Concretely, the label classifier takes the features \mathbf{x} of each piece of information as input and predicts its probability of being 1, i.e., $p(\hat{y} = 1|\mathbf{x})$. Given that only source domain information is labeled, the label classifier is trained using labelled source domain information. The covariate alignment module trains a domain classifier to predict whether a piece of information is from a source domain or the target domain. As the objective of this module is to alleviate the feature distribution difference between source domains and the target domain, the domain classifier is trained to be perplexed in distinguishing between source domain information and target domain information (Ganin et al. 2016).

Proposition 1 sheds light on the design of the concept alignment module, the main innovation of our method. According to the proposition, for each piece of information in a source domain, we need to find its nearest target domain information. Therefore, it is imperative to have a function that measures the similarity between two pieces of information over their feature space. To this end, we introduce a contrastive learning sub-module that learns a similarity function using labeled source domain information. Utilizing the similarity function, a concept alignment sub-module identifies the nearest target domain information for each piece of source domain information. By Proposition 1, this sub-module then mitigates concept shift between source domains and the target domain by minimizing $\sum_{j=1}^k \sum_{i=1}^{N_{S_j}} |f_{S_j}(\mathbf{x}_i^{S_j}) - f_T(c(\mathbf{x}_i^{S_j}))|$, where $f_{S_j}(\mathbf{x}_i^{S_j})$ and $f_T(c(\mathbf{x}_i^{S_j}))$ are estimated using the label classifier in the classification module.

4.3. Classification Module and Covariate Alignment Module

As depicted in Figure 1, the classification module and the covariate alignment module share a feature transformation layer. This layer, denoted by F_h , takes each feature vector \mathbf{x} in $X^{S_1}, X^{S_2}, \dots, X^{S_k}, X^T$ as input and outputs the transformed vector \mathbf{h} . Formally, we have

$$\mathbf{h} = F_h(\mathbf{x}) = \text{MLP}_1(\mathbf{x}; \theta_h), \quad (5)$$

where MLP_1 is a multi-layer perceptron (MLP) with trainable parameters θ_h .

The classification module features an MLP-based label classifier, denoted by F_y , which takes the transformed feature vector \mathbf{h} as input and outputs the probability of being labeled as 1 (i.e., false) for the piece of information characterized by feature vector \mathbf{x} . Concretely, we have

$$p(\hat{y} = 1|\mathbf{x}) = F_y(\mathbf{h}) = \text{Sigmoid}(\text{MLP}_2(\mathbf{h}; \theta_y)), \quad (6)$$

where \hat{y} is the predicted label for the piece of information, MLP_2 is an MLP with trainable parameters θ_y , and $\text{Sigmoid}()$ denotes the sigmoid function. The classification module is trained by minimizing the total cross-entropy loss summed over all labeled source domain information:

$$\begin{aligned} \mathcal{L}_y(\theta_h, \theta_y) &= - \sum_{\mathbf{x} \in X^S} \left[y \log(p(\hat{y} = 1|\mathbf{x})) + (1 - y) \log(1 - p(\hat{y} = 1|\mathbf{x})) \right] \\ &= - \sum_{\mathbf{x} \in X^S} \left[y \log F_y(F_h(\mathbf{x})) + (1 - y) \log(1 - F_y(F_h(\mathbf{x}))) \right], \end{aligned} \quad (7)$$

where $X^S = \cup_{j=1}^k X^{S_j}$ and y is the true label of \mathbf{x} . Minimizing \mathcal{L}_y trains the classification module to score high probabilities for true labels, thereby inducing a model with low source error (i.e., $\sum_{j=1}^k \epsilon_{S_j}(h)$ in Proposition 1).

The covariate alignment module aims to mitigate covariate shift between source domains and the target domain, i.e., reducing $\sum_{j=1}^k \hat{d}_{\mathcal{H}}(\mathcal{D}_{S_j}, \mathcal{D}_T)$ in Proposition 1. To this end, we adapt the domain adversarial method developed by Ganin et al. (2016) to implement this module. Let d denote the true domain for a piece of information characterized by feature vector \mathbf{x} , where $d = 0$ if it belongs to a source domain and $d = 1$ if it comes from the target domain. The module employs a domain classifier, denoted by F_d , that takes the transformed feature vector \mathbf{h} as input and outputs its probability of belonging to the target domain. Mathematically, we have

$$p(\hat{d} = 1|\mathbf{x}) = F_d(\mathbf{h}) = \text{Sigmoid}(\text{MLP}_3(\mathbf{h}; \theta_d)), \quad (8)$$

where \hat{d} is the predicted domain (i.e., source or target) for \mathbf{x} , and MLP_3 is an MLP with trainable parameters θ_d . On the one hand, F_d is trained to accurately predict the domain for each piece of information. On the other hand, to reduce covariate shift, the vector \mathbf{h} produced by the feature transformation layer F_h should be domain-invariant, i.e., when presented to F_d , the classifier cannot tell whether it is from a source domain or the target domain (Li et al. 2021). With this reasoning in mind, the learning of domain-invariant features can be formulated as a min-max game defined as follows (Ganin et al. 2016, Li et al. 2021):

$$\begin{aligned} & \min_{\theta_h} \max_{\theta_d} \sum_{\mathbf{x} \in X} \left[d \log(p(\hat{d} = 1|\mathbf{x})) + (1 - d) \log(1 - p(\hat{d} = 1|\mathbf{x})) \right] \\ & = \min_{\theta_h} \max_{\theta_d} \sum_{\mathbf{x} \in X} \left[d \log F_d(F_h(\mathbf{x})) + (1 - d) \log(1 - F_d(F_h(\mathbf{x}))) \right], \end{aligned} \quad (9)$$

where $X = (\cup_{j=1}^k X^{S_j}) \cup X^T$ and d is the true domain (i.e., source or target) that \mathbf{x} belongs to. The maximization objective in Equation 9 promotes a more accurate domain classifier, while the minimization objective strengthens the domain invariance of the transformed feature vector \mathbf{h} by making hard even for the most accurate domain classifier to discern its domain identity. Following Ganin et al. (2016), the two adversarial objectives in Equation 9 can be unified using a gradient reversal layer $R(\mathbf{z})$ defined as:

$$R(\mathbf{z}) = \mathbf{z}; \frac{dR(\mathbf{z})}{d\mathbf{z}} = -\mathbf{I}, \quad (10)$$

where \mathbf{I} is an identity matrix. According to Equation 10, the gradient reversal layer makes no change to its input but flips the sign of the gradient passed through it. Equipped with the gradient reversal layer, solving the min-max problem in Equation 9 is equivalent to minimize the following loss (Ganin et al. 2016):

$$\mathcal{L}_d(\theta_h, \theta_d) = - \sum_{\mathbf{x} \in X} \left[d \log F_d(R(F_h(\mathbf{x}))) + (1 - d) \log(1 - F_d(R(F_h(\mathbf{x})))) \right], \quad (11)$$

where we replace $F_h(\mathbf{x})$ in Equation 9 with $R(F_h(\mathbf{x}))$. To minimize the loss defined in Equation 11, parameters θ_d of the domain classifier F_d are updated with gradient descent, leading to a more accurate domain classifier. In contrast, because of the gradient reversal layer, parameters θ_h of the feature transformation layer F_h are adjusted with gradient ascent, resulting in more domain-invariant \mathbf{h} (Ganin et al. 2016).

4.4. Concept Alignment Module

The key novelty of our method is the proposed concept alignment module, which mitigates concept shift between source domains and the target domain. By Proposition 1, to mitigate concept shift, we need to learn a function that measures the similarity between two pieces of information. To this end, we propose a contrastive learning sub-module. Specifically, for two pieces of information respectively characterized by feature vectors \mathbf{x}_i and \mathbf{x}_j , we define the similarity between them as

$$F_s(\mathbf{x}_i, \mathbf{x}_j) = \frac{\text{MLP}_4(\mathbf{x}_i; \theta_s) \cdot \text{MLP}_4(\mathbf{x}_j; \theta_s)}{\|\text{MLP}_4(\mathbf{x}_i; \theta_s)\| \|\text{MLP}_4(\mathbf{x}_j; \theta_s)\|}, \quad (12)$$

where F_s denotes the similarity function, MLP_4 is an MLP with learnable parameters θ_s that transforms a feature vector (e.g., \mathbf{x}_i) into a different representation space, notation \cdot denotes the dot product of two vectors, and $\|\cdot\|$ represents the L^2 norm of a vector.

According to Equation 12, learning the similarity function F_s is essentially learning the parameters θ_s of MLP_4 . The rationale underlying the learning is that information with identical labels exhibit greater similarity than information with distinct labels in their representation space (Frosst et al. 2019). Therefore, we design the contrastive learning sub-module that learns the parameters θ_s via the objective of maximizing the similarity between identically labeled information in the transformed representation space while minimizing the similarity between distinctly labeled information. More specifically, for each piece of source domain information characterized by feature vector \mathbf{x} , we randomly select another piece of source domain information, bearing the same label, as its positive peer. We denote the feature vector of the positive peer as \mathbf{x}^+ . In addition, we randomly select m other pieces of source domain information, each having the opposite label of the focal information characterized by \mathbf{x} , to serve as its negative peers. We denote the feature vectors of these negative peers as \mathbf{x}_l^- , $l = 1, 2, \dots, m$. The objective is thus to maximize the similarity $F_s(\mathbf{x}, \mathbf{x}^+)$ between \mathbf{x} and \mathbf{x}^+ , while minimizing the similarity $F_s(\mathbf{x}, \mathbf{x}_l^-)$ between \mathbf{x} and \mathbf{x}_l^- , $l = 1, 2, \dots, m$. Accordingly, the contrastive learning sub-module learns the similarity function by minimizing the following loss summed over all labelled source domain information:

$$\mathcal{L}_s(\theta_s) = - \sum_{\mathbf{x} \in X^S} \log \frac{\exp(F_s(\mathbf{x}, \mathbf{x}^+)/\tau)}{\exp(F_s(\mathbf{x}, \mathbf{x}^+)/\tau) + \sum_{l=1}^m \exp(F_s(\mathbf{x}, \mathbf{x}_l^-)/\tau)}, \quad (13)$$

where $X^S = \cup_{j=1}^k X^{S_j}$, F_s is given in Equation 12, and $0 < \tau < 1$ is a hyperparameter.¹⁰ By minimizing \mathcal{L}_s w.r.t. θ_s , this sub-module learns F_s that measures the similarity between two pieces of information in their transformed representation space such that identically labeled information are close to each other and distinctly labeled information are distant from each other.

Applying the similarity function F_s , for each piece of source domain information characterized by feature vector $\mathbf{x}_i^{S_j}$, the concept alignment sub-module identifies its most similar target domain information characterized by feature vector $c(\mathbf{x}_i^{S_j})$, $j = 1, 2, \dots, k$ and $i = 1, 2, \dots, N_{S_j}$. It then mitigates concept shift between source domains and the target domain by minimizing $\sum_{j=1}^k \sum_{i=1}^{N_{S_j}} |f_{S_j}(\mathbf{x}_i^{S_j}) - f_T(c(\mathbf{x}_i^{S_j}))|$ in Proposition 1. To this end, $f_{S_j}(\mathbf{x}_i^{S_j})$ and $f_T(c(\mathbf{x}_i^{S_j}))$ are estimated using the label classifier described in Section 4.3. Specifically, we have

$$\hat{f}_{S_j}(\mathbf{x}_i^{S_j}) = p(\hat{y} = 1 | \mathbf{x}_i^{S_j}) = F_y(F_h(\mathbf{x}_i^{S_j})),$$

where \hat{f}_{S_j} is the estimation of f_{S_j} , and F_h and F_y are defined by Equations 5 and 6, respectively. Similarly, $f_T(c(\mathbf{x}_i^{S_j}))$ is estimated by

$$\hat{f}_T(c(\mathbf{x}_i^{S_j})) = p(\hat{y} = 1 | c(\mathbf{x}_i^{S_j})) = F_y(F_h(c(\mathbf{x}_i^{S_j}))).¹¹$$

With the estimations of f_{S_j} and f_T , the concept alignment sub-module reduces concept shift by minimizing $\sum_{j=1}^k \sum_{i=1}^{N_{S_j}} |F_y(F_h(\mathbf{x}_i^{S_j})) - F_y(F_h(c(\mathbf{x}_i^{S_j})))|$. Accordingly, this sub-module is trained by minimizing the following loss:

$$\mathcal{L}_c(\theta_h, \theta_y) = \sum_{\mathbf{x} \in X^S} \left[(F_y(F_h(\mathbf{x})) - F_y(F_h(c(\mathbf{x}))))^2 - (F_y(F_h(\mathbf{x})) - F_y(F_h(d(\mathbf{x}))))^2 \right]. \quad (14)$$

where $X^S = \cup_{j=1}^k X^{S_j}$. For each piece of source domain information with feature vector $\mathbf{x} \in X^S$, $c(\mathbf{x})$ and $d(\mathbf{x})$ respectively denote the feature vectors characterizing its most similar and most dissimilar target domain information, both of which are identified using the similarity function F_s . Minimizing the first term in \mathcal{L}_c essentially minimizes $\sum_{j=1}^k \sum_{i=1}^{N_{S_j}} |F_y(F_h(\mathbf{x}_i^{S_j})) - F_y(F_h(c(\mathbf{x}_i^{S_j})))|$. Consequently, it enforces the desired property that similar source and target domain information have similar label predictions (Liu et al. 2022), thus reducing concept shift between source domains and the target domain. Minimizing the second term $-(F_y(F_h(\mathbf{x})) - F_y(F_h(d(\mathbf{x}))))^2$ maximizes the label prediction difference between $F_y(F_h(\mathbf{x}))$ and $F_y(F_h(d(\mathbf{x})))$. As a result, label predictions diverge for dissimilar source and target domain information, which further mitigates concept shift.

¹⁰ Hyperparameter τ adjusts the emphasis on the two objectives (Frosst et al. 2019). Lower τ enables the learning of the similarity function to place more emphasis on maximizing $F_s(\mathbf{x}, \mathbf{x}^+)$ while higher τ shifts the learning to emphasize more on minimizing $F_s(\mathbf{x}, \mathbf{x}^-)$.

¹¹ The label classifier is trained to minimize the error of classifying source domain information. Thus, it is reasonable to estimate f_{S_j} using the label classifier. Since target domain information is unlabeled, we proxy f_T using the label classifier, a strategy of which the effectiveness has been validated by previous studies (Long et al. 2013, 2018, Tachet des Combes et al. 2020).

4.5. The DACA Method

The DACA method is trained to minimize the combined losses of its three modules:

$$\mathcal{L}_{\text{DACA}}(\theta_h, \theta_y, \theta_d, \theta_s) = \mathcal{L}_y(\theta_h, \theta_y) + \mathcal{L}_d(\theta_h, \theta_d) + \mathcal{L}_s(\theta_s) + \mathcal{L}_c(\theta_h, \theta_y) \quad (15)$$

where \mathcal{L}_y , \mathcal{L}_d , \mathcal{L}_s , and \mathcal{L}_c are defined by Equations 7, 11, 13, and 14, respectively. There are two practical considerations when training DACA. First, the DACA method is trained in a two-stage manner. In the first stage (or the warmup stage), the method is trained by minimizing $\mathcal{L}_{\text{DACA}} - \mathcal{L}_c$. The rationale is that, to accurately estimate the concept alignment loss \mathcal{L}_c , DACA needs to learn a reliable similarity function first. In the second stage, DACA is trained by minimizing $\mathcal{L}_{\text{DACA}}$ as defined by Equation 15. Second, to speed up the training of the DACA method, it is beneficial to mitigate concept shift between each pair of source domains. This is accomplished by minimizing a loss function for each pair of source domains. Concretely, for a pair of source domains S_j and S_n , the loss function has the same form as Equation 14 but with S_j treated as the source domain in the equation and S_n regarded as the target domain. Once trained, DACA predicts the probability that a piece of target domain information characterized by feature vector \mathbf{x}_T is false as $F_y(F_h(\mathbf{x}_T))$, where F_h and F_y are defined by Equations 5 and 6, respectively.

5. Empirical Evaluation

5.1. Data

We evaluated the performance of our proposed DACA method using the publicly available datasets of English news, which have been widely employed to assess the performance of misinformation detection methods (Nan et al. 2021, Mosallanezhad et al. 2022, Zhu et al. 2023). One is the MM-COVID dataset, which contains 4,750 pieces of true news (i.e., true information) and 1,317 pieces of fake news (i.e., misinformation) on COVID-19 as well as user comments on these news (Li et al. 2020). Specifically, 8% of COVID news are accompanied by user comments. In our evaluation, we treated the COVID domain as the infodemic or target domain. For source domains, we utilized the FakeNewsNet dataset, which consists of true and fake news alongside their associated comments from the domains of entertainment and politics (Shu et al. 2020). Specifically, there are 16,804 pieces of true news and 5,067 pieces of fake news from the entertainment domain, and 1,583 instances of true news and 1,287 instances of fake news from the politics domain. User comments accompany 27% of entertainment news and 59% of politics news. Table 2 reports the summary statistics of the datasets used in our evaluation. Examples of true and fake news from the source and target domains are given in Figure 2.

5.2. Evaluation Procedure and Benchmark Methods

We considered two scenarios of early detection of misinformation in our evaluation. During the early stage of an infodemic, there is little understanding of the disease that causes the infodemic. Consequently, even experts encounter difficulty distinguishing true news from fake news in the infodemic domain, leaving all

Table 2 Summary Statistics of Evaluation Datasets.

Domain	Number of true news	Number of fake news
COVID (Infodemic / Target)	4,750	1,317
Entertainment (Source)	16,804	5,067
Politics (Source)	1,583	1,287

COVID – True news

News content: Across San Francisco, trips to workplaces, parks, transit stations, and stores have collectively fallen to about 40% of normal levels since late February, as the region and then state enacted strict social distancing measures to halt the spread of the coronavirus. . . .

User comment: wow, how did I miss this? Nice piece!

COVID – Fake news

News content: To prevent the spread of COVID-19, the Centers for Disease Control and Prevention (CDC) now recommends that Americans wear wearing cloth masks in public settings where other social distancing measures are difficult to maintain. . . .

No user comments.

Entertainment – True news

News content: Update: Michael Phelps defended his Shark Week finale episode that left some viewers lukewarm on Sunday. . . .

User comment: Seriously who cares how he did it. Doesn't change he's an Olympic gold medalist.

Politics – Fake news

News content: The state of Florida can now be added to the growing list of US states that have past bills to legalize the use marijuana. . . .

User comment: This is not accurate.

Figure 2 Examples of True and Fake News in Evaluation Datasets

news in this domain unlabeled. Hence, the first evaluation scenario entails each method (ours or benchmark) utilizing labeled news in the entertainment and politics domains to predict the label for each piece of news in the COVID domain. Accordingly, the inputs to each method encompass labeled news in the entertainment and politics domains, along with user comments on these news, as well as *unlabeled* news in the COVID domain and their associated comments. In the second evaluation scenario, user comments accompanying COVID news are dropped from the inputs. As a result, the inputs in this scenario consist of labeled news in the entertainment and politics domains, alongside user comments on these news, and *unlabeled* news in the COVID domain. This scenario emulates the onset of an infodemic, characterized by a large volume of information, yet with very few or no comments accompanying these information.

In each evaluation scenario, we conducted 25 experiments for every method (ours or benchmark) and measured its performance using the metrics recall and F1-score. To curb the spread of fake news and minimize their societal impact, it is crucial to identify as many instances of fake news as possible (Zhu et al. 2023). To this end, recall is an important metric as it measures the effectiveness of a method in identifying fake news. In addition, F1-score evaluates a method's performance in both identifying fake

news and avoiding predicting true news as fake. Concretely, let P be the number of fake news, TP be the number of fake news that are predicted as fake, and FP be the number of true news that are predicted as fake. Recall is defined as TP/P , and F1-score is computed as $2TP/(TP + FP + P)$.

As reviewed in Section 2 and summarized in Table 1, among all existing misinformation detection methods, only cross-domain misinformation detection methods with unlabeled target domain information can solve the EDM problem investigated in this paper. Therefore, we benchmarked our method against state-of-the-art methods in this category. Specifically, one benchmark is the MMD method, which minimizes covariate shift between source and target domain information, measured using the maximum mean discrepancy (MMD) metric (Huang et al. 2021). Another benchmark is the contrastive adaptation network for misinformation detection (CANMD) method, which assesses covariate shift using a variant of the MMD metric (Yue et al. 2022). In addition, we also compared our method against the domain adversarial neural network (DANN) method; it minimizes covariate shift by learning domain-invariant features from source and target domain information (Li et al. 2021). Moreover, general-purpose domain adaptation methods that were not originally designed for misinformation detection can also be adapted to solve our problem. As analyzed in Section 2.2, there are two categories of domain adaptation methods. One category explicitly measures and minimizes covariate shift while the other category implicitly minimizes covariate shift by learning domain-invariant features. Accordingly, we benchmarked against representative methods in each category. For the category that explicitly measures and minimizes covariate shift, we considered the multi-kernel MMD (MK-MMD) method (Long et al. 2015), the joint adaptation network (JAN) method (Long et al. 2017), and the discriminator-free adversarial learning network (DALN) method (Chen et al. 2022) as our baselines. MK-MMD and JAN (Long et al. 2015, 2017) are commonly used domain adaption methods whereas DALN (Chen et al. 2022) is a state-of-the-art method in this category. Representative methods in the other category include the maximum classifier discrepancy (MCD) method (Saito et al. 2018) and the smooth domain adversarial training (SDAT) method (Rangwani et al. 2022). MCD is widely used for domain adaptation and SDAT is a state-of-the-art implicit domain adaptation method. Table 3 lists all methods compared in our evaluation.

In each evaluation scenario, all compared methods took identical inputs and employed the same content embedding method to represent the textual contents of these inputs. Specifically, English words in the inputs were embedded using the pretrained Roberta model (Liu et al. 2019). Next, the content embedding method proposed by Zhu et al. (2023) was utilized to embed the textual contents of the inputs. This method was developed based on BERT (Kenton and Toutanova 2019) and extracted three types of features from each instance of textual content (e.g., a news article): (1) semantic features, such as word usage patterns, (2) style features, such as writing styles, and (3) emotional features, such as emotional signals expressed in a news article. It then aggregated these features into a single feature vector through an attention mechanism. We trained our DACA method using the Adam optimizer with a learning rate of 0.0001 (Kingma and Ba 2015).

Table 3 Methods Compared in Our Evaluation.

Method	Notes
DACA	Our method
MMD	Cross-domain misinformation detection method based on the MMD metric (Huang et al. 2021)
CANMD	Cross-domain misinformation detection method based on a variant of the MMD metric (Yue et al. 2022)
DANN	Cross-domain misinformation detection method based on the learning of domain-invariant features (Li et al. 2021)
MK-MMD	Domain adaptation method based on the multi-kernel MMD metric (Long et al. 2015)
JAN	Domain adaptation method based on the joint MMD metric (Long et al. 2017)
DALN	Domain adaptation method using the Nuclear-norm Wasserstein Discrepancy (Chen et al. 2022)
MCD	Domain adaptation method utilizing a mini-max mechanism to align feature distributions between source and target domains (Saito et al. 2018)
SDAT	Domain adaptation method employing a smoothing mechanism to learn domain-invariant features (Rangwani et al. 2022)

The hyperparameters in Equation 13 of our method were set as follows: the number of instances of source domain information m was set to 3, and the hyperparameter τ was set to 0.5. Implementation details of the benchmark methods are given in Appendix C.

5.3. Evaluation Results

Table 4 presents the average recall and F1-score for each method in evaluation scenario 1, along with standard deviations (in parentheses), across 25 experiments. As reported, our DACA method significantly outperforms each benchmark method in both recall and F1-score. In particular, our method achieves an average recall of 0.745, indicating that, on average, it correctly identifies 74.5% of fake news in the COVID domain. Such performance is attained without any labeled COVID news in the training data, highlighting the efficacy of our method in transferring a model learned from labeled news in the entertainment and politics domains to predict the labels of news in the COVID domain. Moreover, our method respectively outperforms three state-of-the-art misinformation detection methods—MMD, CANMD, and DANN—by 5.82%, 6.13%, and 13.22% in recall, and by 6.05%, 8.77%, and 10.62% in F1-score. Additionally, the performance advantages of our method over representative domain adaptation methods—MK-MMD, JAN, DALN, MCD, and SDAT—range from 4.20% to 11.36% in recall and from 4.66% to 18.26% in F1-score. Since the key methodological difference between our method and the benchmark methods lies in the mitigation of concept shift by its concept alignment module, the performance improvements achieved by our method can be largely attributed to this module. Given the huge volume of information generated at the early stage of an infodemic, such performance advantages

achieved by our method could result in substantially more instances of misinformation being identified by our method, in comparison to the benchmarks. As a result, a greater volume of misinformation could be prevented from dissemination, thereby significantly benefiting public health and society at large (Buchanan 2020, Van Der Linden 2022).

Table 4 Performance Comparison between Our Method and Benchmark Methods (Evaluation Scenario 1).

Method	Recall	Improvement by DACA	F1-score	Improvement by DACA
DACA	0.745 (0.049)		0.719 (0.034)	
MMD	0.704** (0.044)	5.82%	0.678** (0.049)	6.05%
CANMD	0.702** (0.026)	6.13%	0.661** (0.030)	8.77%
DANN	0.658** (0.053)	13.22%	0.650** (0.047)	10.62%
MK-MMD	0.715* (0.038)	4.20%	0.687** (0.041)	4.66%
JAN	0.710** (0.030)	4.93%	0.686** (0.034)	4.81%
DALN	0.669** (0.039)	11.36%	0.660** (0.052)	7.47%
MCD	0.671** (0.020)	11.03%	0.608** (0.049)	18.26%
SDAT	0.712** (0.002)	4.63%	0.682** (0.015)	5.43%

Note: Significance levels are denoted by * and ** for 0.05 and 0.01, respectively.

Table 5 reports the average recall and F1-score for each method in evaluation scenario 2, with standard deviations given in parentheses. Again, our method significantly outperforms each benchmark method in both evaluation metrics. Specifically, it surpasses three state-of-the-art misinformation detection methods with recall improvements ranging from 6.15% to 17.00% and F1-score enhancements ranging from 5.47% to 13.92%. Moreover, in comparison to five representative domain adaptation methods, our method boosts recall by a range of 4.73% to 12.74% and increases F1-score by a range of 4.13% to 13.47%.¹² As a robustness check, we conducted another empirical evaluation using a public dataset of Chinese news. Evaluation results reported in Appendix D further support the superior performance of our method over the benchmarks.

¹² For each method, its performance change in two evaluation scenarios is small because only 8% of COVID news is accompanied by user comments. Further, different methods respond differently to noises and signals in user comments. As a result, dropping user comments associated with COVID news leads to decreased performance for some methods and improved performance for others.

Table 5 Performance Comparison between Our Method and Benchmark Methods (Evaluation Scenario 2).

Method	Recall	Improvement by DACA	F1-score	Improvement by DACA
DACA	0.757 (0.019)		0.720 (0.021)	
MMD	0.713** (0.048)	6.15%	0.682** (0.046)	5.47%
CANMD	0.701** (0.031)	7.89%	0.657** (0.033)	9.59%
DANN	0.647** (0.038)	17.00%	0.632** (0.039)	13.92%
MK-MMD	0.722** (0.031)	4.73%	0.691** (0.033)	4.13%
JAN	0.710** (0.026)	6.63%	0.680** (0.036)	5.79%
DALN	0.671** (0.040)	12.74%	0.661** (0.043)	8.87%
MCD	0.679** (0.021)	11.50%	0.633** (0.025)	13.47%
SDAT	0.695** (0.025)	8.80%	0.665** (0.035)	8.20%

Note: Significance levels are denoted by * and ** for 0.05 and 0.01, respectively.

5.4. Performance Analysis

Having demonstrated the superior performance of our method over the benchmarks, it is intriguing to delve deeper and analyze the factors contributing to its performance advantages. To this end, we conducted ablation studies to investigate the contribution of each novel design artifact of our DACA method to its performance. In particular, we focused on the key novelty of our method – the concept alignment module. As elaborated in Section 4.4, it consists of two sub-modules: the contrastive learning sub-module and the concept alignment sub-module. The former represents instances of information in a transformed space, whereas the latter computes distances between these instances in the transformed space and mitigates concept shift. To evaluate the overall contribution of the concept alignment module, we removed this module from the DACA method and designated the resulting method as W/o_CL_CA (Without both the Contrastive Learning and the Concept Alignment sub-modules). The performance difference between DACA and W/o_CL_CA reveals the overall contribution of the concept alignment module to the performance of our method. To further investigate the functioning mechanism of the concept alignment module, we dropped its contrastive learning sub-module but kept its concept alignment sub-module. We named the resulting method W/o_CL (Without the Contrastive Learning sub-module). The performance difference between DACA and W/o_CL uncovers the role of the contrastive learning sub-module in concept alignment.

Table 6 Ablation Study of DACA (Evaluation Scenario 1).

Method	Recall	Improvement by DACA	F1-score	Improvement by DACA
DACA	0.745 (0.049)		0.719 (0.034)	
W/o_CL_CA	0.658** (0.053)	13.22%	0.650** (0.047)	10.62%
W/o_CL	0.663** (0.047)	12.37%	0.648** (0.052)	10.96%

Note: Significance level is denoted by ** for 0.01.

Table 7 Ablation Study of DACA (Evaluation Scenario 2).

Method	Recall	Improvement by DACA	F1-score	Improvement by DACA
DACA	0.757 (0.019)		0.720 (0.021)	
W/o_CL_CA	0.647** (0.038)	17.00%	0.632** (0.039)	13.92%
W/o_CL	0.663** (0.034)	14.18%	0.638** (0.025)	12.85%

Note: Significance level is denoted by ** for 0.01.

Table 6 presents the average performance of DACA, W/o_CL_CA, and W/o_CL in evaluation scenario 1, along with their respective standard deviations (in parentheses), across 25 experiments. As reported, the performance of W/o_CL_CA is significantly inferior to that of DACA, due to the removal of the concept alignment module. More specifically, W/o_CL_CA trails DACA by 13.22% in recall and 10.62% in F1-score, which collectively demonstrate the contribution of the concept alignment module to the performance of DACA. Furthermore, W/o_CL performs significantly worse than DACA but comparable to W/o_CL_CA. It is noted that W/o_CL has the concept alignment sub-module while omitting the contrastive learning sub-module. The comparison results thus show that, to realize the benefits of the concept alignment sub-module, it must be coupled with the contrastive learning sub-module. This empirical finding is in line with the theoretical analysis in Section 4.1, which defines concept shift over source domain instances and their corresponding nearest target domain instances. Therefore, to mitigate concept shift, we need a suitable similarity function that measures similarities between instances in an appropriate representation space. And the similarity function is learned by the contrastive learning sub-module. Table 7 reports the results of the ablation study in evaluation scenario 2, consistent with our findings from the ablation study in evaluation scenario 1. Overall, the ablation studies in both scenarios demonstrate the significant contribution of its

concept alignment module to the performance of our method. Moreover, the ablation studies show that it is appropriate to design this module with two sub-modules: contrastive learning and concept alignment.

6. Conclusions

6.1. Summary and Contributions

To contain harmful effects of an infodemic on public health, it is crucial to detect misinformation at the early stage of the infodemic. An early stage infodemic is characterized by a large volume of unlabeled information spread across various media platforms. Consequently, conventional misinformation detection methods are not suitable for this misinformation detection task because they rely on labeled information in the infodemic domain to train their models. State-of-the-art misinformation detection methods learn their models with labeled information in other domains to detect misinformation in the infodemic domain, thereby applicable to the task. The efficacy of these methods depends on their ability to mitigate both covariate shift and concept shift between the infodemic domain and the domains from which they leverage labeled information. These methods focus on mitigating covariate shift but overlook concept shift, making them less effective for the task. In response, we propose a novel misinformation detection method that addresses both covariate shift and concept shift. Through extensive empirical evaluations with two widely used datasets, we demonstrate the superior performance of our method over state-of-the-art misinformation detection methods as well as prevalent domain adaptation methods that can be tailored to solve the misinformation detection task.

Our study makes the following contributions to the extant literature. First, our study belongs to the area of computational design science research in the Information Systems (IS) field (Rai et al. 2017, Padmanabhan et al. 2022). This area of research develops computational algorithms and methods to solve business and societal problems and aims at making methodological contributions to the literature, e.g., Abbasi et al. (2010), Li et al. (2017), Zhao et al. (2023). In particular, the methodological contribution of our study lies in its addressing of concept shift, in addition to covariate shift. More specifically, we theoretically show the importance of addressing concept shift and how to operationalize it. Built on the theoretical analysis, we develop a novel concept alignment module to mitigate concept shift, as described in Section 4.4. Second, given its significant social and economic impact, misinformation detection and management has attracted attention from IS scholars, e.g., Moravec et al. (2019), Wei et al. (2022), Hwang and Lee (2024). Our study adds to this stream of IS research with a novel method that is effective in detecting misinformation at the early stage of an infodemic.

6.2. Implications for Infodemic Management and Future Work

Every epidemic is accompanied by an infodemic, a phenomenon known since the Middle Ages (Zarocostas 2020). The wide dissemination of misinformation during an infodemic misleads people to dismiss health guidance and pursue unscientific treatments, resulting in substantial harm to public health and significant social and economic consequences (Bursztyn et al. 2020, Romer and Jamieson 2020).

Furthermore, the pervasive reach of the Internet and social media platforms accelerates the spread of misinformation and amplifies its harmful impacts on public health and society (Zarocostas 2020). Detecting misinformation at the early stage of an infodemic discourages people from believing and sharing it, thereby preventing it from going viral (Buchanan 2020). Hence, early detection of misinformation is crucial for managing an infodemic and mitigating its adverse effects. Accordingly, a direct implication of our study is to provide an effective early misinformation detection method for infodemic management. Our method effectively overcomes obstacles to early detection of misinformation. First, vast amount of information spread during the early stage of an infodemic makes manual identification of misinformation impractical. In response, our deep learning-based method automatically learns to differentiate misinformation from true information. Second, there is no labeled information at the early stage of an infodemic, rendering traditional misinformation detection methods inapplicable. Accordingly, our method leverages labeled information in other domains to detect misinformation in the infodemic domain.

Our study empowers infodemic management in several ways. Operators of media platforms can employ our method to effectively detect misinformation in the infodemic domain that spreads on their platforms. Subsequently, they can flag and debunk identified misinformation, which helps curb the diffusion of misinformation and alleviate its negative impacts (Pennycook et al. 2020, Wei et al. 2022). Additionally, flagged misinformation is less likely to be clicked, thereby reducing revenues for those who monetize misinformation and diminishing their incentives to create more misinformation (Pennycook and Rand 2021). Moreover, platform operators can trace misinformation identified by our method back to its producers. They could then restrict those who frequently produce misinformation from publishing on their platforms. In this regard, platforms are encouraged to set up guidelines to regulate their content producers (Hartley and Vu 2020). Platform operators can also trace misinformation detected by our method to its spreaders. Understandably, blocking individuals who disseminate a large amount of misinformation is important for combating misinformation on their platforms.

Furthermore, our study sheds light on the value of cross-domain data sharing for infodemic management. At the early stage of an infodemic, even experts have difficulty in distinguishing between misinformation and true information. Moreover, recruiting experts to verify and label information is costly (Kim et al. 2018). Cross-domain data sharing enables us to utilize labeled information in other domains to detect misinformation in the infodemic domain. Hence, it is a viable and cost-effective approach to misinformation detection and infodemic management. To implement this approach, we need to address a challenge. Information from different domains exhibits different marginal and conditional distributions, known as covariate shift and concept shift, respectively. Thus, the challenge is how to mitigate covariate shift and concept shift between the infodemic domain and source domains that provide labeled information. Our proposed DACA method is effective in tackling this challenge. To facilitate cross-domain data sharing for infodemic management, media platforms are recommended to establish data exchange

mechanisms to ensure that participating platforms are properly incentivized and labeled information is securely shared.

Our study has limitations and can be extended in several directions. First, our method employs information content to detect misinformation. Future work could extend our method by incorporating information propagation patterns. To this end, graphical neural networks are useful tools for modeling such patterns. Second, our empirical evaluations are based on fake news datasets, which have been widely utilized to assess the performance of misinformation detection methods in the literature. It is also interesting to evaluate the performance of our method in detecting other types of misinformation such as hyperpartisan news and yellow journalism (Pennycook and Rand 2021). Third, our method could be generalized to solve other domain adaptation problems, in addition to the misinformation detection problem tackled in this study. Hence, another area worthy of future investigation is how to generalize our method to solve the problem of classifying unlabeled target domain instances by leveraging labeled source domain instances.

References

- Abbasi A, Zhang Z, Zimbra D, Chen H, Nunamaker Jr JF (2010) Detecting fake websites: The contribution of statistical learning theory. *MIS Quarterly* 435–461.
- Adebimpe WO, Adeyemi DH, Faremi A, Ojo JO, Efuntoye AE (2015) The relevance of the social networking media in ebola virus disease prevention and control in southwestern nigeria. *The Pan African Medical Journal* 22(Suppl 1).
- Agrahari S, Singh AK (2022) Concept drift detection in data stream mining: A literature review. *Journal of King Saud University-Computer and Information Sciences* 34(10):9523–9540.
- Arjovsky M, Chintala S, Bottou L (2017) Wasserstein generative adversarial networks. *Proceedings of the 34th International Conference on Machine Learning*, 214–223.
- Asadi K, Misra D, Littman M (2018) Lipschitz continuity in model-based reinforcement learning. *Proceedings of the 35th International Conference on Machine Learning*, 264–273 (PMLR).
- Atanasov P, Rescober P, Stone E, Swift SA, Servan-Schreiber E, Tetlock P, Ungar L, Mellers B (2017) Distilling the wisdom of crowds: Prediction markets vs. prediction polls. *Management Science* 63(3):691–706.
- Ben-David S, Blitzer J, Crammer K, Kulesza A, Pereira F, Vaughan JW (2010) A theory of learning from different domains. *Machine Learning* 79:151–175.
- Borah P, Austin E, Su Y (2022) Injecting disinfectants to kill the virus: Media literacy, information gathering sources, and the moderating role of political ideology on misperceptions about covid-19. *Mass Communication and Society* 1–27.
- Buchanan T (2020) Why do people spread false information online? the effects of message and viewer characteristics on self-reported likelihood of sharing social media disinformation. *Plos one* 15(10):e0239666.
- Bursztyn L, Rao A, Roth CP, Yanagizawa-Drott DH (2020) Misinformation during a pandemic. Technical report, National Bureau of Economic Research.
- Chen L, Chen H, Wei Z, Jin X, Tan X, Jin Y, Chen E (2022) Reusing the task-specific classifier as a discriminator: Discriminator-free adversarial domain adaptation. *Proceedings of the IEEE/CVF Conference on Computer Vision and Pattern Recognition*, 7181–7190.
- Ciampaglia GL, Shiralkar P, Rocha LM, Bollen J, Menczer F, Flammini A (2015) Computational fact checking from knowledge networks. *PloS one* 10(6):e0128193.
- Fang X, Sheng ORL, Goes P (2013) When is the right time to refresh knowledge discovered from data? *Operations Research* 61(1):32–44.
- Freeman D, Waite F, Rosebrock L, Petit A, Causier C, East A, Jenner L, Teale AL, Carr L, Mulhall S, et al. (2022) Coronavirus conspiracy beliefs, mistrust, and compliance with government guidelines in england. *Psychological Medicine* 52(2):251–263.
- Frosst N, Papernot N, Hinton G (2019) Analyzing and improving representations with the soft nearest neighbor loss. *Proceedings of the 36th International Conference on Machine Learning*, 2012–2020 (PMLR).
- Ganin Y, Ustinova E, Ajakan H, Germain P, Larochelle H, Laviolette F, March M, Lempitsky V (2016) Domain-adversarial training of neural networks. *Journal of Machine Learning Research* 17(59):1–35.
- Hartley K, Vu MK (2020) Fighting fake news in the covid-19 era: policy insights from an equilibrium model. *Policy Sciences* 53(4):735–758.
- Huang Y, Gao M, Wang J, Shu K (2021) Dafd: Domain adaptation framework for fake news detection. *Proceedings of the 28th Neural Information Processing Conference*, 305–316.
- Hwang EH, Lee S (2024) A nudge to credible information as a countermeasure to misinformation: Evidence from twitter. *Information Systems Research*.
- Imhoff R, Lambert P (2020) A bioweapon or a hoax? the link between distinct conspiracy beliefs about the coronavirus disease (covid-19) outbreak and pandemic behavior. *Social Psychological and Personality Science* 11(8):1110–1118.
- Kenton JDMWC, Toutanova LK (2019) Bert: Pre-training of deep bidirectional transformers for language understanding. *Proceedings of NAACL-HLT*, 4171–4186.

- Kim H, Papamakarios G, Mnih A (2021) The lipschitz constant of self-attention. Proceedings of the 38th International Conference on Machine Learning, 5562–5571 (PMLR).
- Kim J, Tabibian B, Oh A, Schölkopf B, Gomez-Rodriguez M (2018) Leveraging the crowd to detect and reduce the spread of fake news and misinformation. Proceedings of the eleventh ACM International Conference on Web Search and Data Mining, 324–332.
- Kingma DP, Ba J (2015) Adam: A method for stochastic optimization. Proceedings of the 3rd International Conference on Learning Representations.
- Kouw WM, Loog M (2018) An introduction to domain adaptation and transfer learning. arXiv preprint arXiv:1812.11806.
- Li Y, Jiang B, Shu K, Liu H (2020) Mm-covid: A multilingual and multimodal data repository for combating covid-19 disinformation. arXiv preprint arXiv:2011.04088.
- Li Y, Lee K, Kordzadeh N, Faber B, Fiddes C, Chen E, Shu K (2021) Multi-source domain adaptation with weak supervision for early fake news detection. Proceedings of the 2021 IEEE International Conference on Big Data (Big Data), 668–676 (IEEE).
- Li Z, Fang X, Bai X, Sheng ORL (2017) Utility-based link recommendation for online social networks. Management Science 63(6):1938–1952.
- Liu X, Yoo C, Xing F, Oh H, El Fakhri G, Kang JW, Woo J, et al. (2022) Deep unsupervised domain adaptation: A review of recent advances and perspectives. APSIPA Transactions on Signal and Information Processing 11(1).
- Liu Y, Ott M, Goyal N, Du J, Joshi M, Chen D, Levy O, Lewis M, Zettlemoyer L, Stoyanov V (2019) Roberta: A robustly optimized bert pretraining approach. arXiv preprint arXiv:1907.11692.
- Long M, Cao Y, Wang J, Jordan M (2015) Learning transferable features with deep adaptation networks. Proceedings of the 32nd International Conference on Machine Learning, 97–105 (PMLR).
- Long M, Cao Z, Wang J, Jordan MI (2018) Conditional adversarial domain adaptation. Proceedings of the 32nd International Conference on Neural Information Processing Systems, 1647–1657. NIPS'18 (Red Hook, NY, USA: Curran Associates Inc.).
- Long M, Wang J, Ding G, Sun J, Yu PS (2013) Transfer feature learning with joint distribution adaptation. Proceedings of the IEEE International Conference on Computer Vision, 2200–2207.
- Long M, Zhu H, Wang J, Jordan MI (2017) Deep transfer learning with joint adaptation networks. Proceedings of the 34th International Conference on Machine Learning, 2208–2217 (PMLR).
- Moravec PL, Minas RK, Dennis AR (2019) Fake news on social media: People believe what they want to believe when it makes no sense at all. MIS Quarterly 43(4).
- Mosallanezhad A, Karami M, Shu K, Mancenido MV, Liu H (2022) Domain adaptive fake news detection via reinforcement learning. Proceedings of the ACM Web Conference 2022, 3632–3640.
- Nan Q, Cao J, Zhu Y, Wang Y, Li J (2021) Mdfend: Multi-domain fake news detection. Proceedings of the 30th ACM International Conference on Information & Knowledge Management, 3343–3347.
- Nan Q, Wang D, Zhu Y, Sheng Q, Shi Y, Cao J, Li J (2022) Improving fake news detection of influential domain via domain-and instance-level transfer. Proceedings of the 29th International Conference on Computational Linguistics, 2834–2848.
- Ng KC, Ke PF, So MK, Tam KY (2023) Augmenting fake content detection in online platforms: A domain adaptive transfer learning via adversarial training approach. Production and Operations Management 32(7):2101–2122.
- Oh O, Agrawal M, Rao HR (2013) Community intelligence and social media services: A rumor theoretic analysis of tweets during social crises. MIS Quarterly 407–426.
- Padmanabhan B, Fang X, Sahoo N, Burton-Jones A (2022) Machine learning in information systems research. MIS Quarterly 46(1):iii–xix.
- Papanastasiou Y (2020) Fake news propagation and detection: A sequential model. Management Science 66(5):1826–1846.
- Peng X, Bai Q, Xia X, Huang Z, Saenko K, Wang B (2019) Moment matching for multi-source domain adaptation. Proceedings of the IEEE/CVF International Conference on Computer Vision, 1406–1415.
- Pennycook G, Bear A, Collins ET, Rand DG (2020) The implied truth effect: Attaching warnings to a subset of fake news headlines increases perceived accuracy of headlines without warnings. Management Science 66(11):4944–4957.
- Pennycook G, Rand DG (2021) The psychology of fake news. Trends in Cognitive Sciences 25(5):388–402.
- Rai A, Burton-Jones A, Chen H, Gupta A, Hevner AR, Ketter W, Parsons J, Rao HR, Sarkar S, Yoo Y (2017) Editor's comments: Diversity of design science research. MIS Quarterly 41(1):iii–xviii.
- Rangwani H, Aithal SK, Mishra M, Jain A, Radhakrishnan VB (2022) A closer look at smoothness in domain adversarial training. Proceedings of the 39th International Conference on Machine Learning, 18378–18399 (PMLR).
- Romer D, Jamieson KH (2020) Conspiracy theories as barriers to controlling the spread of covid-19 in the us. Social Science & Medicine 263:113356.
- Rostami M, Galstyan A (2023) Overcoming concept shift in domain-aware settings through consolidated internal distributions. Proceedings of the AAAI Conference on Artificial Intelligence, volume 37, 9623–9631.
- Roychowdhury S, Kasa SR, Gupta K, Murthy PS, Chandra A (2023) Tackling concept shift in text classification using entailment-style modeling. NeurIPS 2023 Workshop on Distribution Shifts: New Frontiers with Foundation Models.
- Saito K, Watanabe K, Ushiku Y, Harada T (2018) Maximum classifier discrepancy for unsupervised domain adaptation. Proceedings of the IEEE Conference on Computer Vision and Pattern Recognition, 3723–3732.
- Shu K, Mahudeswaran D, Wang S, Lee D, Liu H (2020) Fakenewsnet: A data repository with news content, social context, and spatiotemporal information for studying fake news on social media. Big Data 8(3):171–188.
- Siering M, Koch JA, Deokar AV (2016) Detecting fraudulent behavior on crowdfunding platforms: The role of linguistic and content-based cues in static and dynamic contexts. Journal of Management Information Systems 33(2):421–455.
- Tachet des Combes R, Zhao H, Wang YX, Gordon GJ (2020) Domain Adaptation with Conditional Distribution Matching and Generalized Label Shift. Advances in Neural Information Processing Systems, volume 33, 19276–19289 (Curran Associates, Inc.).
- Van Der Linden S (2022) Misinformation: susceptibility, spread, and interventions to immunize the public. Nature Medicine 28(3):460–467.
- Vorburger P, Bernstein A (2006) Entropy-based concept shift detection. Proceedings of the Sixth International Conference on Data Mining, 1113–1118.
- Vosoughi S, Roy D, Aral S (2018) The spread of true and false news online. Science 359(6380):1146–1151.
- Wei X, Zhang Z, Zhang M, Chen W, Zeng DD (2022) Combining crowd and machine intelligence to detect false news on social media. MIS Quarterly 46(2):977–1008.
- Yue Z, Zeng H, Kou Z, Shang L, Wang D (2022) Contrastive domain adaptation for early misinformation detection: A case study on covid-19. Proceedings of the 31st ACM International Conference on Information & Knowledge Management, 2423–2433.

-
- Zajonc RB (2001) Mere exposure: A gateway to the subliminal. Current Directions in Psychological Science 10(6):224–228.
- Zarocostas J (2020) How to fight an infodemic. The lancet 395(10225):676.
- Zhang YF, Wang J, Liang J, Zhang Z, Yu B, Wang L, Tao D, Xie X (2023) Domain-specific risk minimization for domain generalization. Proceedings of the 29th ACM SIGKDD Conference on Knowledge Discovery and Data Mining, 3409–3421.
- Zhao X, Fang X, He J, Huang L (2023) Exploiting expert knowledge for assigning firms to industries: A novel deep learning method. MIS Quarterly 47(3):1147–1176.
- Zhou X, Zafarani R (2020) A survey of fake news: Fundamental theories, detection methods, and opportunities. ACM Computing Surveys (CSUR) 53(5):1–40.
- Zhu Y, Sheng Q, Cao J, Nan Q, Shu K, Wu M, Wang J, Zhuang F (2023) Memory-guided multi-view multi-domain fake news detection. IEEE Trans. Knowl. Data Eng. 35(7):7178–7191.
- Zhu Y, Zhuang F, Wang D (2019) Aligning domain-specific distribution and classifier for cross-domain classification from multiple sources. Proceedings of the AAAI Conference on Artificial Intelligence, volume 33, 5989–5996.

Appendix A \mathcal{H} -divergence

\mathcal{H} -divergence has been widely utilized to measure distances between distributions over a feature space.

Definition A.1. (\mathcal{H} -divergence) (Ben-David et al. 2010). Given a feature space \mathcal{X} , let \mathcal{H} denote a hypothesis space defined on \mathcal{X} and \mathbb{D}_S and \mathbb{D}_T be two probability distributions over \mathcal{X} . For a hypothesis $h \in \mathcal{H}$, let $I(h)$ be the set such that $\mathbf{x} \in I(h)$ if and only if $h(\mathbf{x}) > \tau$, where τ is the classification threshold and an instance with features \mathbf{x} is classified as 1 if $h(\mathbf{x}) > \tau$ and 0 otherwise. The \mathcal{H} -divergence between \mathbb{D}_S and \mathbb{D}_T is defined as

$$d_{\mathcal{H}}(\mathbb{D}_S, \mathbb{D}_T) = 2 \sup_{h \in \mathcal{H}} |Pr_{\mathbb{D}_S}[I(h)] - Pr_{\mathbb{D}_T}[I(h)]|, \quad (\text{A1})$$

where Pr denotes probability.¹³

The \mathcal{H} -divergence between two distributions can be empirically estimated using two sample datasets drawn from these distributions, respectively (Ben-David et al. 2010). Given a dataset of N_S source domain instances \mathcal{D}_S and a dataset of N_T target domain instances \mathcal{D}_T , features of which are from distributions \mathbb{D}_S and \mathbb{D}_T respectively, the \mathcal{H} -divergence between \mathbb{D}_S and \mathbb{D}_T can be estimated using $\hat{d}_{\mathcal{H}}(\mathcal{D}_S, \mathcal{D}_T)$ (Ben-David et al. 2010):

$$\hat{d}_{\mathcal{H}}(\mathcal{D}_S, \mathcal{D}_T) = 2 \left(1 - \min_{h \in \mathcal{H}} \left[\frac{1}{N_S} \sum_{\mathbf{x}: h(\mathbf{x}) \leq \tau} I[\mathbf{x} \in \mathcal{D}_S] + \frac{1}{N_T} \sum_{\mathbf{x}: h(\mathbf{x}) > \tau} I[\mathbf{x} \in \mathcal{D}_T] \right] \right), \quad (\text{A2})$$

where indicator function $I[\mathbf{x} \in \mathcal{D}_S]$ is 1 if an instance with feature \mathbf{x} belongs to \mathcal{D}_S and \mathcal{H} is a symmetric hypothesis space (i.e., for each hypothesis $h \in \mathcal{H}$, its inverse $1 - h$ is also in \mathcal{H}).

Appendix B Proof of Theorem and Proposition

Let $\epsilon_S(g_1, g_2) = E_{\mathbf{x} \sim \mathbb{D}_S}[|g_1(\mathbf{x}) - g_2(\mathbf{x})|]$ be the expected difference between g_1 and g_2 in the source domain, where g_1 and g_2 are two labeling functions. Similarly, $\epsilon_T(g_1, g_2) = E_{\mathbf{x} \sim \mathbb{D}_T}[|g_1(\mathbf{x}) - g_2(\mathbf{x})|]$ denotes the expected difference between g_1 and g_2 in the target domain. To prove Theorem 1, we first show an upper bound of $\epsilon_S(f_S, f_T)$:

Lemma 1 Let f_S and f_T respectively denote the true source and target domain labeling functions, \mathbb{D}_S be the source domain feature distribution, and \mathcal{D}_S be a dataset with N_S samples drawn from \mathbb{D}_S , for any $\eta \in (0, 1)$, the following inequality holds with probability at least $1 - \eta$:

$$\epsilon_S(f_S, f_T) = E_{\mathbf{x} \sim \mathbb{D}_S}[|f_S(\mathbf{x}) - f_T(\mathbf{x})|] \leq \frac{1}{N_S} \sum_{i=1}^{N_S} |f_S(\mathbf{x}_i^S) - f_T(\mathbf{x}_i^S)| + \sqrt{-\frac{\ln(\frac{\eta}{2})}{2N_S}}, \quad (\text{A3})$$

where \mathbf{x}_i^S is the i -th sample drawn i.i.d. from \mathbb{D}_S .

¹³ Ben-David et al. (2010) consider a hypothesis h that produces a discrete output, i.e., 0 or 1, while we consider a hypothesis h that predicts a continuous output between 0 and 1.

Proof. This proof relies on McDiarmid's inequality (Doob 1940). For notation convenience, define $\mathbf{z} = f_S(\mathbf{x}) - f_T(\mathbf{x})$ where $\mathbf{x} \sim \mathbb{D}_S$. We then have $\mathbf{z}_i = f_S(\mathbf{x}_i^S) - f_T(\mathbf{x}_i^S), i = 1, 2, \dots, N_S$. Further define $g(\mathbf{z}_1, \mathbf{z}_2, \dots, \mathbf{z}_{N_S}) = \frac{1}{N_S} \sum_{i=1}^{N_S} |\mathbf{z}_i|$. Function g satisfies the property that

$$|g(\mathbf{z}_1, \mathbf{z}_2, \dots, \mathbf{z}_{N_S}) - g(\mathbf{z}_1, \dots, \mathbf{z}_{k-1}, \mathbf{z}'_k, \mathbf{z}_{k+1}, \dots, \mathbf{z}_{N_S})| \leq \frac{1}{N_S}, \quad (\text{A4})$$

which means that by changing any k -th coordinate, the function will change at most $\frac{1}{N_S}$. This is because $|\mathbf{z}_k| = |f_S(\mathbf{x}_k^S) - f_T(\mathbf{x}_k^S)| \in [0, 1]$.

Given that $\mathbf{z}_1, \mathbf{z}_2, \dots, \mathbf{z}_{N_S}$ are i.i.d. random samples, for any $\epsilon > 0$, by McDiarmid's inequality

$$\begin{aligned} p(|g(\mathbf{z}_1, \mathbf{z}_2, \dots, \mathbf{z}_{N_S}) - E[g(\mathbf{z}_1, \mathbf{z}_2, \dots, \mathbf{z}_{N_S})]| \geq \epsilon) &\leq 2 \exp\left(\frac{-2\epsilon^2}{\sum_{k=1}^{N_S} \frac{1}{N_S^2}}\right) \\ &= 2 \exp(-2N_S\epsilon^2). \end{aligned} \quad (\text{A5})$$

Equivalently,

$$p(|g(\mathbf{z}_1, \mathbf{z}_2, \dots, \mathbf{z}_{N_S}) - E[g(\mathbf{z}_1, \mathbf{z}_2, \dots, \mathbf{z}_{N_S})]| \leq \epsilon) \geq 1 - 2 \exp(-2N_S\epsilon^2). \quad (\text{A6})$$

By replacing ϵ with $\sqrt{-\frac{\ln(\frac{\eta}{2})}{2N_S}}$ where $\eta \in (0, 1)$, we have

$$p\left(|g(\mathbf{z}_1, \mathbf{z}_2, \dots, \mathbf{z}_{N_S}) - E[g(\mathbf{z}_1, \mathbf{z}_2, \dots, \mathbf{z}_{N_S})]| \leq \sqrt{-\frac{\ln(\frac{\eta}{2})}{2N_S}}\right) \geq 1 - \eta, \quad (\text{A7})$$

Note that $E[g(\mathbf{z}_1, \mathbf{z}_2, \dots, \mathbf{z}_{N_S})] = E_{\mathbf{x} \sim \mathbb{D}_S}[|f_S(\mathbf{x}) - f_T(\mathbf{x})|]$ by construction, while $g(\mathbf{z}_1, \mathbf{z}_2, \dots, \mathbf{z}_{N_S}) = \frac{1}{N_S} \sum_{i=1}^{N_S} |f_S(\mathbf{x}_i^S) - f_T(\mathbf{x}_i^S)|$ by definition. Based on the inequality $a - b \leq |b - a|$, Inequality A7 means that Inequality A3 must hold with probability at least $1 - \eta$, which concludes our proof of Lemma 1.

Next, we show, in Lemma 2, that the population \mathcal{H} -divergence is bounded by the empirical \mathcal{H} -divergence.

Lemma 2 Let \mathcal{H} be a hypothesis space with VC dimension d . \mathcal{D}_S and \mathcal{D}_T are datasets of instances drawn from distributions \mathbb{D}_S and \mathbb{D}_T , respectively. Let $d_{\mathcal{H}}(\mathbb{D}_S, \mathbb{D}_T)$ denote the population \mathcal{H} -divergence between distributions \mathbb{D}_S and \mathbb{D}_T , and $\hat{d}_{\mathcal{H}}(\mathcal{D}_S, \mathcal{D}_T)$ be its empirical estimation from datasets \mathcal{D}_S and \mathcal{D}_T . For any $\eta \in (0, 1)$, with probability at least $1 - \eta$,

$$d_{\mathcal{H}}(\mathbb{D}_S, \mathbb{D}_T) \leq \hat{d}_{\mathcal{H}}(\mathcal{D}_S, \mathcal{D}_T) + 4 \max\left\{\sqrt{\frac{d \ln(2N_S) + \ln(\frac{2}{\eta})}{N_S}}, \sqrt{\frac{d \ln(2N_T) + \ln(\frac{2}{\eta})}{N_T}}\right\}, \quad (\text{A8})$$

where N_S is the number of instances in \mathcal{D}_S and N_T is the number of instances in \mathcal{D}_T .

Proof. According to Kifer et al. (2004), we have

$$P\left[\left|d_{\mathcal{H}}(\mathbb{D}_S, \mathbb{D}_T) - \hat{d}_{\mathcal{H}}(\mathcal{D}_S, \mathcal{D}_T)\right| > \epsilon\right] \leq (2N_S)^d e^{-N_S\epsilon^2/16} + (2N_T)^d e^{-N_T\epsilon^2/16}. \quad (\text{A9})$$

By replacing $(2N_S)^d e^{-N_S\epsilon^2/16} + (2N_T)^d e^{-N_T\epsilon^2/16}$ with η , we get

$$\eta \leq 2 \max\{(2N_S)^d e^{-N_S\epsilon^2/16}, (2N_T)^d e^{-N_T\epsilon^2/16}\}, \quad (\text{A10})$$

which means that $\eta \leq 2(2N_S)^d e^{-N_S \epsilon^2/16}$ as well as $\eta \leq 2(2N_T)^d e^{-N_S \epsilon^2/16}$. In other words, we have $\epsilon \leq 4\sqrt{(d\ln(2N_S) + \ln(2/\eta))/N_S}$ as well as $\epsilon \leq 4\sqrt{(d\ln(2N_T) + \ln(2/\eta))/N_T}$. Because increasing ϵ will decrease the probability $P \left[\left| d_{\mathcal{H}}(\mathbb{D}_S, \mathbb{D}_T) - \hat{d}_{\mathcal{H}}(\mathcal{D}_S, \mathcal{D}_T) \right| > \epsilon \right]$, for

$$\epsilon_{\max} = 4 \max \left\{ \sqrt{\frac{d\ln(2N_S) + \ln(\frac{2}{\eta})}{N_S}}, \sqrt{\frac{d\ln(2N_T) + \ln(\frac{2}{\eta})}{N_T}} \right\}, \quad (\text{A11})$$

we have

$$\begin{aligned} \eta &\geq P \left[\left| d_{\mathcal{H}}(\mathbb{D}_S, \mathbb{D}_T) - \hat{d}_{\mathcal{H}}(\mathcal{D}_S, \mathcal{D}_T) \right| > \epsilon \right] \\ &\geq P \left[\left| d_{\mathcal{H}}(\mathbb{D}_S, \mathbb{D}_T) - \hat{d}_{\mathcal{H}}(\mathcal{D}_S, \mathcal{D}_T) \right| > \epsilon_{\max} \right] \end{aligned} \quad (\text{A12})$$

which concludes the proof of Lemma 2. If $N_S = N_T$, Lemma 2 will reduce to Lemma 1 in Ben-David et al. (2010).

Definition A.2. (The ideal hypothesis). The ideal hypothesis h^* is defined as the hypothesis that minimizes the summation of the expected differences between $h \in \mathcal{H}$ and the target domain labeling function f_T in both source and target domains

$$h^* = \arg \min_{h \in \mathcal{H}} \epsilon_S(h, f_T) + \epsilon_T(h, f_T), \quad (\text{A13})$$

where $\epsilon_S(h, f_T) = E_{\mathbf{x} \sim \mathbb{D}_S} [|h(\mathbf{x}) - f_T(\mathbf{x})|]$ and $\epsilon_T(h, f_T) = E_{\mathbf{x} \sim \mathbb{D}_T} [|h(\mathbf{x}) - f_T(\mathbf{x})|]$.

The error incurred by the ideal hypothesis is $\lambda = \epsilon_S(h^*, f_T) + \epsilon_T(h^*, f_T)$. Now, we provide the proof of Theorem 1 utilizing the lemmas established above.

Theorem 1 For a source domain instance with features \mathbf{x}_i^S , let $c(\mathbf{x}_i^S)$ be the features of its nearest target domain instance, where $i = 1, 2, \dots, N_S$ and the distance between a pair of instances are measured over their feature space. If f_T is L -Lipschitz continuous, then for any $\eta \in (0, 1)$, with probability at least $(1 - \eta)^2$,

$$\epsilon_T(h) \leq \epsilon_S(h) + \hat{d}_{\mathcal{H}}(\mathcal{D}_S, \mathcal{D}_T) + \frac{1}{N_S} \sum_{i=1}^{N_S} |f_S(\mathbf{x}_i^S) - f_T(c(\mathbf{x}_i^S))| + \frac{L}{N_S} \sum_{i=1}^{N_S} \|\mathbf{x}_i^S - c(\mathbf{x}_i^S)\| + C_1, \quad (\text{A14})$$

where L is the Lipschitz constraint constant, $\hat{d}_{\mathcal{H}}(\mathcal{D}_S, \mathcal{D}_T)$ denotes the empirical \mathcal{H} -divergence between distributions \mathbb{D}_S and \mathbb{D}_T , $\|\mathbf{x}_i^S - c(\mathbf{x}_i^S)\|$ represents the distance between \mathbf{x}_i^S and $c(\mathbf{x}_i^S)$, and $C_1 = \lambda + \sqrt{-\frac{\ln(\frac{\eta}{2})}{2N_S}} + 2 \max \left\{ \sqrt{\frac{d\ln(2N_S) + \ln(\frac{2}{\eta})}{N_S}}, \sqrt{\frac{d\ln(2N_T) + \ln(\frac{2}{\eta})}{N_T}} \right\}$.

Proof. With probability at least $(1 - \eta)^2$,

$$\begin{aligned}
\epsilon_T(h) &\leq \epsilon_T(h^*) + \epsilon_S(h) + \epsilon_S(h^*) + \frac{1}{2}d_{\mathcal{H}}(\mathbb{D}_S, \mathbb{D}_T) \\
&\leq \epsilon_T(h^*) + \epsilon_S(h) + \epsilon_S(h^*, f_T) + \epsilon_S(f_S, f_T) + \frac{1}{2}d_{\mathcal{H}}(\mathbb{D}_S, \mathbb{D}_T) \\
&= \epsilon_S(h) + \frac{1}{2}d_{\mathcal{H}}(\mathbb{D}_S, \mathbb{D}_T) + \epsilon_S(f_S, f_T) + \lambda \\
&\leq \epsilon_S(h) + \frac{1}{2}\hat{d}_{\mathcal{H}}(\mathcal{D}_S, \mathcal{D}_T) + \frac{1}{N_S} \sum_{i=1}^{N_S} |f_S(\mathbf{x}_i^S) - f_T(\mathbf{x}_i^S)| + C_1 \\
&= \epsilon_S(h) + \frac{1}{2}\hat{d}_{\mathcal{H}}(\mathcal{D}_S, \mathcal{D}_T) + \frac{1}{N_S} \sum_{i=1}^{N_S} |f_S(\mathbf{x}_i^S) + f_T(c(\mathbf{x}_i^S)) - f_T(c(\mathbf{x}_i^S)) - f_T(\mathbf{x}_i^S)| + C_1 \\
&\leq \epsilon_S(h) + \frac{1}{2}\hat{d}_{\mathcal{H}}(\mathcal{D}_S, \mathcal{D}_T) + \frac{1}{N_S} \sum_{i=1}^{N_S} |f_S(\mathbf{x}_i^S) - f_T(c(\mathbf{x}_i^S))| + \frac{1}{N_S} \sum_{i=1}^{N_S} |f_T(c(\mathbf{x}_i^S)) - f_T(\mathbf{x}_i^S)| + C_1 \\
&\leq \epsilon_S(h) + \frac{1}{2}\hat{d}_{\mathcal{H}}(\mathcal{D}_S, \mathcal{D}_T) + \frac{1}{N_S} \sum_{i=1}^{N_S} |f_S(\mathbf{x}_i^S) - f_T(c(\mathbf{x}_i^S))| + \frac{L}{N_S} \sum_{i=1}^{N_S} \|\mathbf{x}_i^S - c(\mathbf{x}_i^S)\| + C_1.
\end{aligned} \tag{A15}$$

The first step is based on the proof of Theorem 2 in Ben-David et al. (2010). The second step is followed by triangle inequality. The third step utilizes the definition $\lambda = \epsilon_S(h^*, f_T) + \epsilon_T(h^*, f_T)$ and the definition $\epsilon_T(h^*) = \epsilon_T(h^*, f_T)$. The fourth step employs Lemma 1 and Lemma 2 to respectively expand the terms $\epsilon_S(f_S, f_T)$ and $d_{\mathcal{H}}(\mathbb{D}_S, \mathbb{D}_T)$ while collecting the constants into C_1 . Because the inequalities given by Lemma 1 and Lemma 2 hold both with at least probability $1 - \eta$, the inequality at the second step holds with at least probability $(1 - \eta)^2$ under the independence assumption. The fifth step adds and subtracts $f_T(c(\mathbf{x}_i^S))$. The sixth step utilizes triangle inequality. The last step is from the assumption of L -Lipschitz continuous for f_T .

By extending Theorem 1 to the case of multiple source domains, we have the following proposition.

Proposition 1 For a source domain instance with features $\mathbf{x}_i^{S_j}$ in \mathcal{D}_{S_j} , let $c(\mathbf{x}_i^{S_j})$ be the features of its nearest instance in \mathcal{D}_T , where $j = 1, 2, \dots, k$ and $i = 1, 2, \dots, N_{S_j}$. If f_T is L -Lipschitz continuous, then for any $\eta \in (0, 1)$, with probability at least $(1 - \eta)^{2k}$,

$$\epsilon_T(h) \leq \frac{1}{k} \sum_{j=1}^k \left\{ \epsilon_{S_j}(h) + \frac{1}{2}\hat{d}_{\mathcal{H}}(\mathcal{D}_{S_j}, \mathcal{D}_T) + \frac{1}{N_{S_j}} \sum_{i=1}^{N_{S_j}} |f_{S_j}(\mathbf{x}_i^{S_j}) - f_T(\mathbf{x}_i^{S_j, T})| + \frac{L}{N_{S_j}} \sum_{i=1}^{N_{S_j}} \|\mathbf{x}_i^{S_j} - \mathbf{x}_i^{S_j, T}\| + C_j \right\}, \tag{A16}$$

where $C_j = \lambda_j + \sqrt{-\frac{\ln(\frac{\eta}{2})}{2N_{S_j}}} + 2 \max\left\{ \sqrt{\frac{d \ln(2N_{S_j}) + \ln(\frac{2}{\eta})}{N_{S_j}}}, \sqrt{\frac{d \ln(2N_T) + \ln(\frac{2}{\eta})}{N_T}} \right\}$, λ_j is the error incurred by the ideal hypothesis $\lambda_j = \epsilon_{S_j}(h^*, f_T) + \epsilon_T(h^*, f_T)$, and L is the constant for the Lipschitz condition.

Proof. By Theorem 1, for any source domain $j = 1, 2, \dots, k$, the following inequality holds with probability at least $(1 - \eta)^2$ for any $\eta \in (0, 1)$,

$$\epsilon_T(h) \leq \epsilon_{S_j}(h) + \hat{d}_{\mathcal{H}}(\mathcal{D}_{S_j}, \mathcal{D}_T) + \frac{1}{N_{S_j}} \sum_{i=1}^{N_{S_j}} |f_{S_j}(\mathbf{x}_i^{S_j}) - f_T(c(\mathbf{x}_i^{S_j}))| + \frac{L}{N_{S_j}} \sum_{i=1}^{N_{S_j}} \|\mathbf{x}_i^{S_j} - c(\mathbf{x}_i^{S_j})\| + C_j. \tag{A17}$$

Proposition 1 follows immediately by summing on each side of inequality (A17) over all source domains.

Appendix C Implementation Details of Benchmark Methods

MMD. Maximum Mean Discrepancy (MMD) is a metric to measure the discrepancy between distributions in a reproducing kernel Hilbert space (RKHS) (Borgwardt et al. 2006). Specifically, a kernel function k is associated with a feature map ϕ , i.e., $k(\mathbf{x}_S, \mathbf{x}_T) = \langle \phi(\mathbf{x}_S), \phi(\mathbf{x}_T) \rangle$, where \mathbf{x}_S and \mathbf{x}_T are source and target distributions. Let \mathcal{H} be an RKHS, and MMD is defined as the discrepancy between the mean embeddings of source and target distributions in \mathcal{H} :

$$\text{MMD} = d(p_S, p_T)^2 = \left\| \frac{1}{N_S} \phi(\mathbf{x}_S) - \frac{1}{N_T} \phi(\mathbf{x}_T) \right\|_{\mathcal{H}}^2. \quad (\text{A18})$$

As reviewed in Section 2.2, MMD is an explicit metric that measures the discrepancy between source and target domains in terms of their feature distributions. In our implementation, we utilized the Gaussian kernel $k(\mathbf{x}_S, \mathbf{x}_T) = e^{-\|\mathbf{x}_S - \mathbf{x}_T\|/\gamma}$ and set $\gamma = 0.5$.

CANMD. Contrastive Adaptation Network for Early Misinformation Detection (CANMD) is a domain adaptation method devised for misinformation detection (Yue et al. 2022). This method assigns pseudo labels to target domain instances. Let D_{ij} denote the multi-kernel MMD discrepancy between the covariate distribution of source domain instances with label i and that of target domain instances with pseudo label j , where $i, j \in \{0, 1\}$. To minimize the divergence between source and target domains, the loss is defined as

$$\mathcal{L} = D_{00} + D_{11} - \frac{1}{2}(D_{01} + D_{10}). \quad (\text{A19})$$

Following Yue et al. (2022), we implemented the multi-kernel MMD using 5 Gaussian kernels with $k(\mathbf{x}_S, \mathbf{x}_T) = e^{-\|\mathbf{x}_S - \mathbf{x}_T\|/\gamma}$ and $\gamma = 2^k$, where the value of k for each Gaussian kernel was set to -3, -2, -1, 0, and 1, respectively. The Gaussian kernels were combined with equal weights.

DANN. The Domain Adversarial Neural Networks (DANN) method has two classifiers: a label classifier and a domain classifier (Ganin et al. 2016, Li et al. 2021). The former is learned to classify each piece of source or target domain information as true or false. The latter is used to learn domain-invariant features. The hyperparameter λ of DANN controls the relative weight between its domain and label classifiers. In our evaluation, we performed a grid search for the value of λ from 1 to 10, with an interval of 1. We found that $\lambda = 5$ yielded the best performance for DANN and chose $\lambda = 5$ accordingly.

MK-MMD. Multi-kernel MMD (MK-MMD) is an extension of single-kernel MMD (Long et al. 2015). Instead of using a single kernel function, MK-MMD employs a convex combination of multiple kernel functions. In our implementation, we used Gaussian kernels $k(\mathbf{x}_S, \mathbf{x}_T) = e^{-\|\mathbf{x}_S - \mathbf{x}_T\|/\gamma}$ and $\gamma = 2^k$, where the value of k for each Gaussian kernel was set to -3, -2, -1, 0, and 1, respectively. The Gaussian kernels were combined with equal weights.

JAN. Joint Adaptation Networks (JAN) measures the discrepancy between source and target domains at each layer of its classifier using MK-MMD (Long et al. 2017). It then combines these discrepancies and minimizes the aggregated discrepancy. The implementation of MK-MMD in JAN is the same as the implementation of MK-MMD described above.

DALN. Discriminator-free Adversarial Learning Network (DALN) utilizes the Nuclear-norm Wasserstein Discrepancy (NWD) to measure the covariate shift (Chen et al. 2022). To compute NWD, Chen et al. (2022) devise a domain classifier that predicts the probability of an instance belonging to the source domain. NWD is then defined as the difference between the average probability of source domain instances and that of target domain instances. The DALN method minimizes the covariate shift by minimizing NWD. In addition, the DALN method has a label classifier that predicts the label (true or false) for each instance. The loss of the method is a summation of NWD and the label classification loss.

MCD. The Maximum Classifier Discrepancy (MCD) method consists of three steps (Saito et al. 2018). In the first step, it trains two classifiers using labeled source domain instances. Next, it maximizes the discrepancy between two classifiers when applied to target domain instances. In the third step, it adjusts its feature extractor to minimize such discrepancy. MCD can be viewed as a generative adversarial network (GAN), with the feature extractor serving as the generator and the two classifiers functioning as the discriminator.

SDAT. Smooth Domain Adversarial Training (SDAT) is an implicit domain adaptation method based on DANN (Rangwani et al. 2022). Inspired by the observation that the label classifier of DANN often falls into sharp minima, Rangwani et al. (2022) devise a smooth training loss based on the Sharpness Aware Minimization (SAM) proposed by Foret et al. (2021). In our implementation, we set the neighborhood size ρ in SAM to 0.05 by following (Foret et al. 2021).

Appendix D Additional Empirical Evaluation

Table A1 Summary Statistics of Chinese News Dataset.

Domain	Number of true news	Number of fake news
COVID (Infodemic / Target)	201	124
Entertainment (Source)	1000	440
Politics (Source)	306	546

We conducted an additional empirical evaluation using a public dataset of Chinese news (Nan et al. 2021). The dataset contains true and fake news in nine different domains. We employed news in three of these domains: entertainment, politics, and health, consistent with the setting of the empirical study with English news datasets. Not all news in the health domain are related to infodemic. We specifically chose

Table A2 Performance Comparison between Our Method and Benchmark Methods using Chinese News Dataset (Evaluation Scenario 1).

Method	Recall	Improvement by DACA	F1-score	Improvement by DACA
DACA	0.836 (0.004)		0.824 (0.010)	
MMD	0.804** (0.006)	3.88%	0.797** (0.001)	3.33%
CANMD	0.792** (0.013)	5.52%	0.789** (0.012)	8.77%
DANN	0.713** (0.002)	17.25%	0.709** (0.001)	16.20%
MK-MMD	0.786** (0.006)	6.33%	0.780** (0.009)	5.64%
JAN	0.723** (0.014)	15.49%	0.718** (0.023)	14.70%
DALN	0.764** (0.013)	9.45%	0.763** (0.002)	7.95%
MCD	0.667** (0.074)	25.33%	0.658** (0.082)	25.12%
SDAT	0.777** (0.002)	7.52%	0.772** (0.008)	6.66%

Note: Significance levels are denoted by * and ** for 0.05 and 0.01, respectively.

news articles from this domain that contain words associated with the COVID pandemic, such as COVID, COVID test, or pandemic. Table A1 lists the number of true and fake news in each domain. User comments accompany 53.22% of COVID news, 84.27% of politics news, and 94.64% of entertainment news.

We followed the same evaluation procedure as described in Section 5.2, except that Chinese words in the dataset were embedded using the pretrained BERT-wwm model (Cui et al. 2021). Table A2 compares the performance between our method and each benchmark method in evaluation scenario 1. As reported, our method significantly outperforms each benchmark, improving recall by a range of 3.88% to 25.33% and increasing F1-score by a range of 3.33% to 25.12%. Table A3 presents the evaluation results of each method in evaluation scenario 2. Again, our method attains significantly better performance than each benchmark method in both recall and F1-score. The additional empirical analysis further confirms the effectiveness of our method in leveraging labeled information in other domains to detect misinformation in the infodemic domain.

Table A3 Performance Comparison between Our Method and Benchmark Methods using Chinese News Dataset (Evaluation Scenario 2).

Method	Recall	Improvement by DACA	F1-score	Improvement by DACA
DACA	0.834 (0.030)		0.818 (0.029)	
MMD	0.793** (0.024)	5.10%	0.786** (0.024)	4.12%
CANMD	0.781** (0.036)	6.74%	0.776** (0.035)	5.45%
DANN	0.686** (0.024)	21.48%	0.671** (0.040)	22.02%
MK-MMD	0.769** (0.019)	8.47%	0.758** (0.019)	7.94%
JAN	0.722** (0.036)	15.42%	0.708** (0.035)	15.55%
DALN	0.706** (0.040)	18.09%	0.710** (0.040)	15.28%
MCD	0.643** (0.004)	29.74%	0.642** (0.006)	27.50%
SDAT	0.744** (0.059)	12.03%	0.741** (0.057)	10.44%

Note: Significance levels are denoted by * and ** for 0.05 and 0.01, respectively.

References

- Ben-David S, Blitzer J, Crammer K, Kulesza A, Pereira F, Vaughan JW (2010) A theory of learning from different domains. *Machine Learning* 79:151–175.
- Borgwardt KM, Gretton A, Rasch MJ, Kriegel HP, Schölkopf B, Smola AJ (2006) Integrating structured biological data by kernel maximum mean discrepancy. *Bioinformatics* 22(14):e49–e57.
- Chen L, Chen H, Wei Z, Jin X, Tan X, Jin Y, Chen E (2022) Reusing the task-specific classifier as a discriminator: Discriminator-free adversarial domain adaptation. *Proceedings of the IEEE/CVF Conference on Computer Vision and Pattern Recognition*, 7181–7190.
- Cui Y, Che W, Liu T, Qin B, Yang Z (2021) Pre-training with whole word masking for chinese bert. *IEEE/ACM Transactions on Audio, Speech, and Language Processing* 29:3504–3514.
- Doob JL (1940) Regularity properties of certain families of chance variables. *Transactions of the American Mathematical Society* 47(3):455–486.
- Foret P, Kleiner A, Mobahi H, Neyshabur B (2021) Sharpness-aware minimization for efficiently improving generalization. *9th International Conference on Learning Representations, ICLR 2021, Virtual Event, Austria, May 3-7, 2021* (OpenReview.net).
- Ganin Y, Ustinova E, Ajakan H, Germain P, Larochelle H, Laviolette F, March M, Lempitsky V (2016) Domain-adversarial training of neural networks. *Journal of Machine Learning Research* 17(59):1–35.
- Kifer D, Ben-David S, Gehrke J (2004) Detecting change in data streams. *VLDB*, volume 4, 180–191 (Toronto, Canada).
- Li Y, Lee K, Kordzadeh N, Faber B, Fiddes C, Chen E, Shu K (2021) Multi-source domain adaptation with weak supervision for early fake news detection. *2021 IEEE International Conference on Big Data (Big Data)*, 668–676 (IEEE).
- Long M, Cao Y, Wang J, Jordan M (2015) Learning transferable features with deep adaptation networks. *Proceedings of the 32nd International Conference on Machine Learning*, 97–105 (PMLR).
- Long M, Zhu H, Wang J, Jordan MI (2017) Deep transfer learning with joint adaptation networks. *Proceedings of the 34th International Conference on Machine Learning*, 2208–2217 (PMLR).
- Nan Q, Cao J, Zhu Y, Wang Y, Li J (2021) Mdfend: Multi-domain fake news detection. *Proceedings of the 30th ACM International Conference on Information & Knowledge Management*, 3343–3347.
- Rangwani H, Aithal SK, Mishra M, Jain A, Radhakrishnan VB (2022) A closer look at smoothness in domain adversarial training. *Proceedings of the 39th International Conference on Machine Learning*, 18378–18399 (PMLR).
- Saito K, Watanabe K, Ushiku Y, Harada T (2018) Maximum classifier discrepancy for unsupervised domain adaptation. *Proceedings of the IEEE Conference on Computer Vision and Pattern Recognition*, 3723–3732.
- Yue Z, Zeng H, Kou Z, Shang L, Wang D (2022) Contrastive domain adaptation for early misinformation detection: A case study on covid-19. *Proceedings of the 31st ACM International Conference on Information & Knowledge Management*, 2423–2433.